Fast Electron Transport in Warm and Hot Dense Plasmas

Farhat Beg

Center for Energy Research & Department of Mechanical and Aerospace Engineering
University of California, San Diego

9th Omega Laser Users Workshop
Laboratory for Laser Energetics
26 - 28 April 2017

This work was performed under the auspices of U.S. DOE under contracts DE-FC02-04ER54789 (FSC), DE-FG02-05ER54834 (ACE) and DE-NA0000854 (NLUF).

High Energy Density Physics Research at UCSD

- High intensity laser matter interactions
  - Relativistic electron transport in solid and warm dense targets
  - Proton production, conversion efficiency and focusing
  - Modeling with LSP, PICLS, ZUMA and Hydra codes

- Mono-energetic ion beams with ultra-intense lasers

- Shock Ignition

- Z-pinches
  - X-ray Thomson Scattering of pulsed power driven plasmas
  - Magnetic field measurement using proton deflectometry
  - Supersonic jets and collisionless shocks
  - Liner physics

- X-pinches
  - Point projection radiography
  - Laser cut x-pinches as rep. rate source
  - Intense source for diagnostics calibration

Recent Publications

nature physics LETTERS
PUBLISHED ONLINE: 4 DECEMBER 2011 | DOI: 10.1038/NPHYS2153

Focusing of short-pulse high-intensity laser-accelerated proton beams

Teresa Bartal[1,2], Mark E. Foord[2], Claudio Bellei[2], Michael H. Key[2], Kirk A. Flippo[3], Sandrine A. Gaillard[4], Dustin T. Offermann[3], Pravesh K. Patel[2], Leonard C. Jarrott[1], Drew P. Higginson[1,2], Markus Roth[5], Anke Otten[5], Dominik Kraus[5], Richard B. Stephens[6], Harry S. McLean[2], Emilio M. Giraldez[6], Mingsheng S. Wei[6], Donald C. Gautier[3] and Farhat N. Beg[1]*

Recent progress in generating high-energy (>50 MeV) protons from intense laser–matter interactions (10^{18}–10^{21} W cm^{-2}; refs 1–7) has opened up new areas of research, with applications in radiography[8], oncology[9], astrophysics[10], medical imaging[11], high-energy-density physics[12–14], and ion-proton beam fast ignition[15–19]. With the discovery of proton focusing with curved surfaces[20,21], rapid advances in these areas will be driven by improved focusing technologies. Here we report on the first investigation of the generation and focusing of a proton beam using a cone-shaped target. We clearly show that the focusing is strongly affected by the electric fields in the beam in both open and enclosed (cone) geometries, bending the trajectories near the axis. Also in the cone geometry, a sheath electric field effectively 'channels' the proton beam through the cone tip, substantially improving the beam focusing properties. These results agree well with particle simulations and provide the physics basis for many future applications.

The ability to generate high-intensity well-focused proton beams of cone-in-shell compression[23] without a hohlraum, where the cone acts both as a guide for the ignitor beam as well as a shield. The properties of the proton beam in this particular geometry require careful examination, especially as the viability of proton FI requires both focusing at the compressed fuel between 20 and 40 μm (refs 16,18), depending on the model, and a conversion efficiency of ≈15% from petawatt laser pulse energy to proton beam energy[9,18]. Studies have shown efficiencies approaching the requirement for FI (refs 6,7,24) and proton focusing from an open geometry curved foil has been demonstrated by laser irradiation of hemispherical Al shells[20,21]. Control of divergent proton beams in flat-foil experiments has been shown using electrostatic fields when the beams pass through charged secondary[25] or attached[26] structures, and better control of the beam divergence has recently been reported in a cylindrical thick-foil geometry[27]. Here we present the first demonstration of the generation and focusing of a proton beam in a FI geometry, where the beam is generated from a curved focusing surface, which propagates and is channelled via surface fields through an enclosed

PRL 108, 115004 (2012) PHYSICAL REVIEW LETTERS week ending 16 MARCH 2012

Hot Electron Temperature and Coupling Efficiency Scaling with Prepulse for Cone-Guided Fast Ignition

T. Ma,[1,2] H. Sawada,[2] P. K. Patel,[1] C. D. Chen,[1] L. Divol,[1] D. P. Higginson,[1,2] A. J. Kemp,[1] M. H. Key,[1] D. J. Larson,[1] S. Le Pape,[1] A. Link,[1,3] A. G. MacPhee,[1] H. S. McLean,[1] Y. Ping,[1] R. B. Stephens,[4] S. C. Wilks,[1] and F. N. Beg[2]
[1]*Lawrence Livermore National Laboratory, Livermore, California 94550, USA*
[2]*University of California-San Diego, La Jolla, California 92093, USA*
[3]*The Ohio State University, Columbus, Ohio 43210, USA*
[4]*General Atomics, San Diego, California 92186, USA*
(Received 3 December 2011; published 16 March 2012)

The effect of increasing prepulse energy levels on the energy spectrum and coupling into forward-going electrons is evaluated in a cone-guided fast-ignition relevant geometry using cone-wire targets irradiated with a high intensity (10^{20} W/cm^2) laser pulse. Hot electron temperature and flux are inferred from $K\alpha$ images and yields using hybrid particle-in-cell simulations. A two-temperature distribution of hot electrons was required to fit the full profile, with the ratio of energy in a higher energy (MeV) component increasing with a larger prepulse. As prepulse energies were increased from 8 mJ to 1 J, overall coupling from laser to all hot electrons entering the wire was found to fall from 8.4% to 2.5% while coupling into only the 1–3 MeV electrons dropped from 0.57% to 0.03%.

DOI: 10.1103/PhysRevLett.108.115004 PACS numbers: 52.50.Jm, 52.38.Kd, 52.38.Mf, 52.70.La

Fast Ignition (FI) [1,2] is an approach to inertial confinement fusion (ICF) in which a precompressed comparison, as the absorption mechanisms would be different for the very different $I\lambda^2$. In the MacPhee *et al.*

PRL 110, 025001 (2013) PHYSICAL REVIEW LETTERS week ending 11 JANUARY 2013

Effect of Target Material on Fast-Electron Transport and Resistive Collimation

S. Chawla,[1,3] M. S. Wei,[2,*] R. Mishra,[1] K. U Akli,[2] C. D. Chen,[3] H. S. McLean,[3] A. Morace,[1,4] P. K. Patel,[3] H. Sawada,[1] Y. Sentoku,[5] R. B. Stephens,[2] and F. N. Beg[1]
[1]*Center for Energy Research, University of California, San Diego, La Jolla, California 92093, USA*
[2]*General Atomics, P.O. Box 85608, San Diego, California 92186, USA*
[3]*Lawrence Livermore National Laboratory, Livermore, California 94551, USA*
[4]*Department of Physics, University of Milano Bicocca, Milano 20126, Italy*
[5]*Department of Physics, University of Nevada, Reno, Nevada 89557, USA*
(Received 27 July 2012; published 7 January 2013)

The effect of target material on fast-electron transport is investigated using a high-intensity (0.7 ps, 10^{20} W/cm^2) laser pulse irradiated on multilayered solid Al targets with embedded transport (Au, Mo, Al) and tracer (Cu) layers, backed with millimeter-thick carbon foils to minimize refluxing. We consistently observed a more collimated electron beam (36% average reduction in fast-electron induced Cu $K\alpha$ spot size) using a high- or mid-Z (Au or Mo) layer compared to Al. All targets showed a similar electron flux level in the central spot of the beam. Two-dimensional collisional particle-in-cell simulations showed formation of strong self-generated resistive magnetic fields in targets with a high-Z transport layer that suppressed the fast-electron beam divergence; the consequent magnetic channels guided the fast electrons to a smaller spot, in good agreement with experiments. These findings indicate that fast-electron transport can be controlled by self-generated resistive magnetic fields and may have important implications to fast ignition.

DOI: 10.1103/PhysRevLett.110.025001 PACS numbers: 52.38.Dx, 52.38.Hb, 52.50.Jm, 52.65.Rr

Cone-guided fast-ignition (FI) inertial confinement fusion requires efficient energy transport of high-intensity short-pulse-laser-produced relativistic (or "fast") electrons through a solid cone tip to a high-density fuel core forward energy coupling, but it is consistent with the analytical model and 2D Fokker-Planck modeling showing stronger resistive collimation in high-Z plasmas by Bell and Kingham [4]. In addition, the collimation did not rely

nature physics ARTICLES
PUBLISHED ONLINE: 11 JANUARY 2016 | DOI: 10.1038/NPHYS3614

Visualizing fast electron energy transport into laser-compressed high-density fast-ignition targets

L. C. Jarrott[1]†, M. S. Wei[2]*, C. McGuffey[1], A. A. Solodov[3,4], W. Theobald[3], B. Qiao[1], C. Stoeckl[3], R. Betti[3,4], H. Chen[5], J. Delettrez[3], T. Döppner[5], E. M. Giraldez[2], V. Y. Glebov[3], H. Habara[6], T. Iwawaki[6], M. H. Key[5], R. W. Luo[2], F. J. Marshall[3], H. S. McLean[5], C. Mileham[3], P. K. Patel[5], J. J. Santos[7], H. Sawada[8], R. B. Stephens[2], T. Yabuuchi[6] and F. N. Beg[1]*

Recent progress in kilojoule-scale high-intensity lasers has opened up new areas of research in radiography, laboratory astrophysics, high-energy-density physics, and fast-ignition (FI) laser fusion. FI requires efficient heating of pre-compressed high-density fuel by an intense relativistic electron beam produced from laser-matter interaction. Understanding the details of electron beam generation and transport is crucial for FI. Here we report on the first visualization of fast electron spatial

Motivation

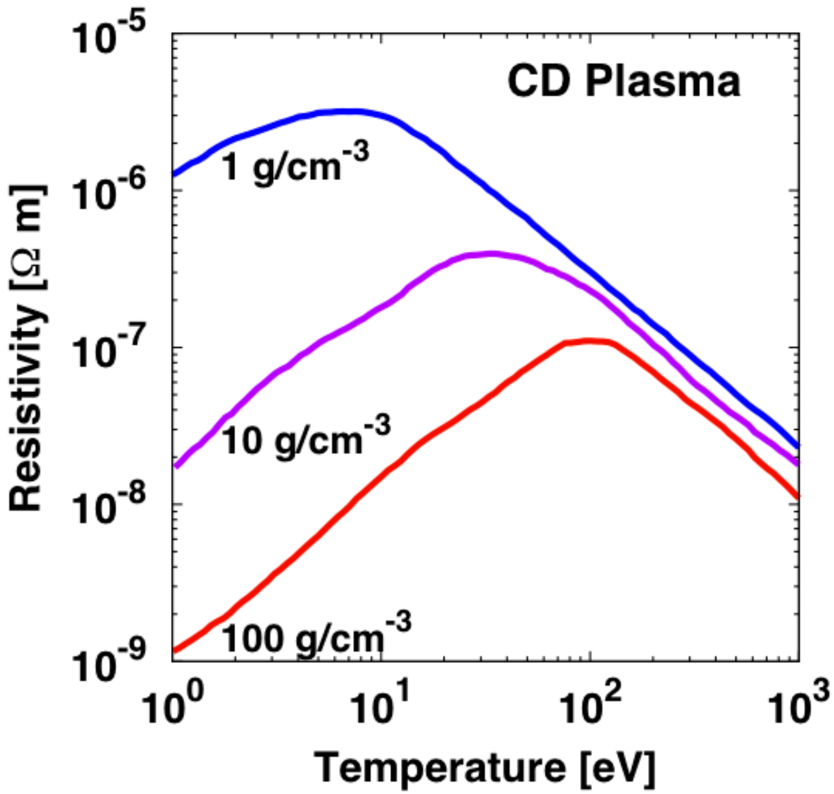

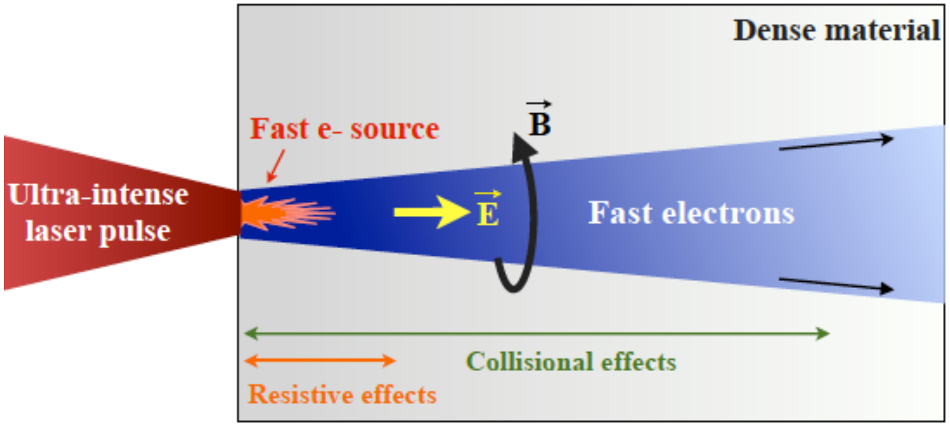

$$\partial \vec{B}_z / \partial t = \underbrace{\eta(\partial \vec{J}_x / \partial y)}_{\text{focusing}} + \underbrace{(\partial \eta / \partial y)\vec{J}_x}_{\text{de-focusing}}$$

- **Fast electron beam propagating into dense medium produces dynamic azimuthal magnetic field, which can affect the beam propagation**

How the target conditions, especially in the 1-100 eV range, affect electron transport?

Outline

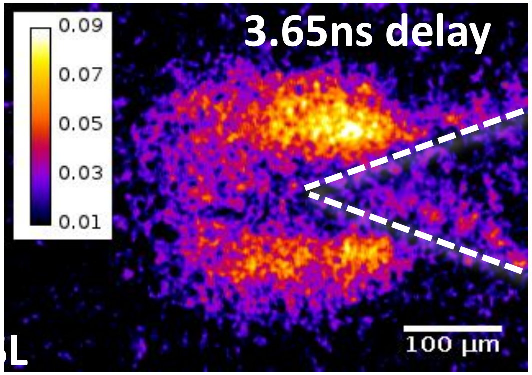

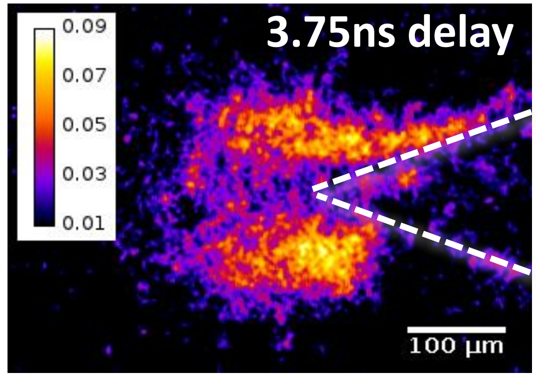

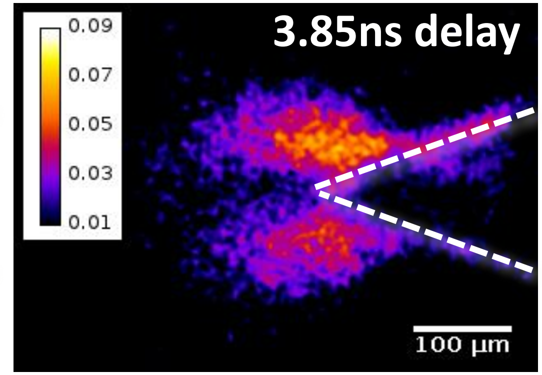

CH Plasma
30 mg/cm^3
360 µm

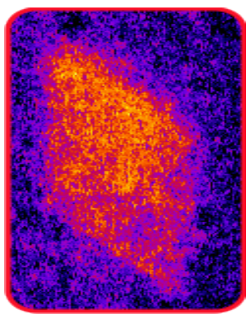

Cold CH
Solid1 g/cm^3
50 µm

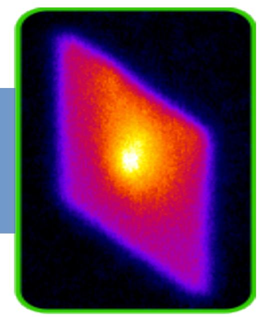

Cold CH
Foam
200 mg/cm^3
250 µm

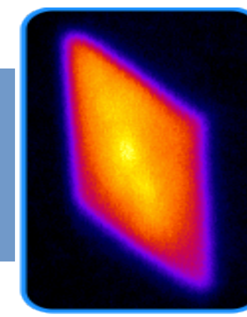

Un-driven HDC

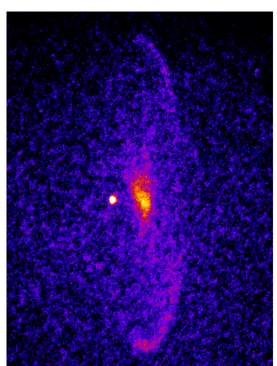

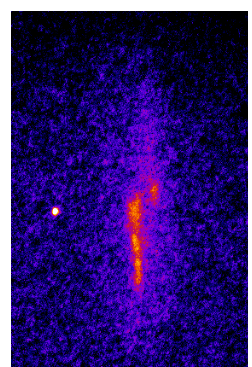

Un-driven VC

There has been a mystery about low energy coupling in high density compressed plasmas

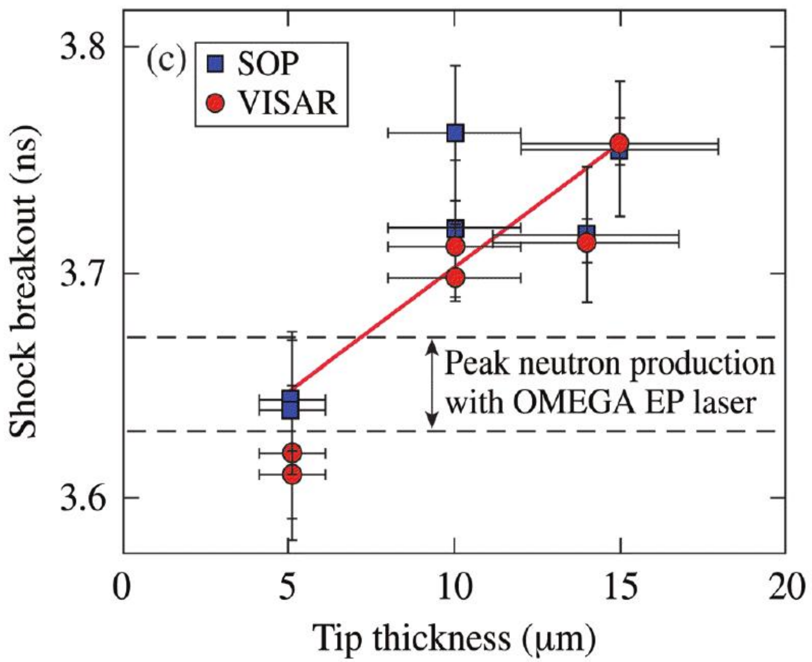

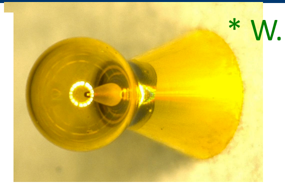

* W. Theobald et al., Phys. Plasmas 18, 056305 (2011)

CD shell:
40 µm thick,
OD 870 µm
Au cone:
34° opening
15 µm thick
10 µm tip dia.

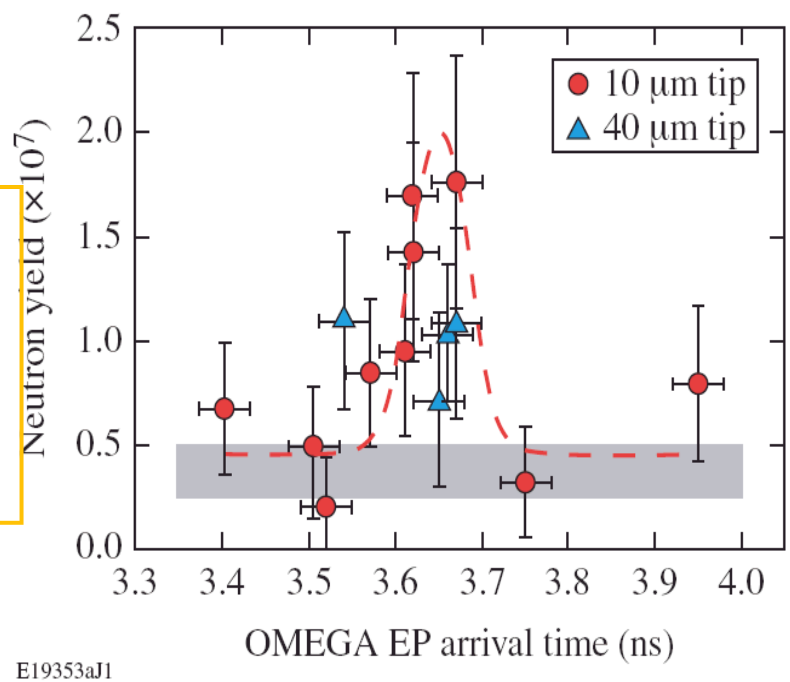

- 18 kJ OMEGA UV driver pulse compresses the shell and 1kJ OMEGA-EP injected into cone at cone-tip
- Varied delay between driver beams and ignition beam to observe enhancements in neutron yield
- Enhancement in neutron yield with short pulse injection

What are the core issues for lower coupling?

CD shell with Cu dopant is used to characterize EP laser produced fast electron transport

X-ray radiography image of
Cone-in-(Cu-doped) CD shell target

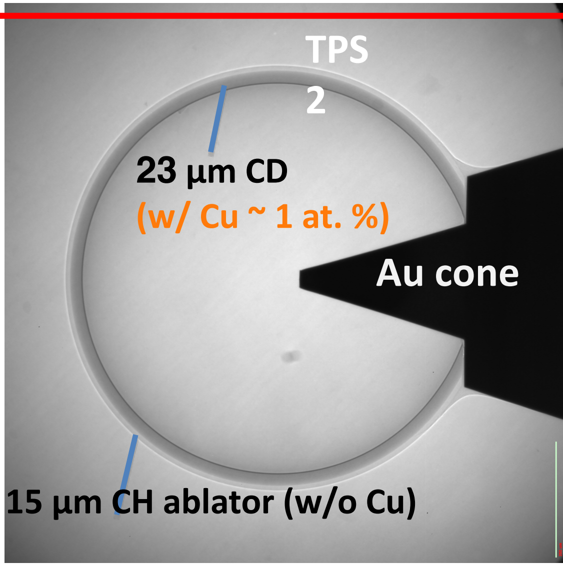

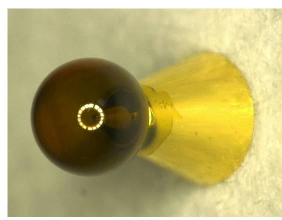

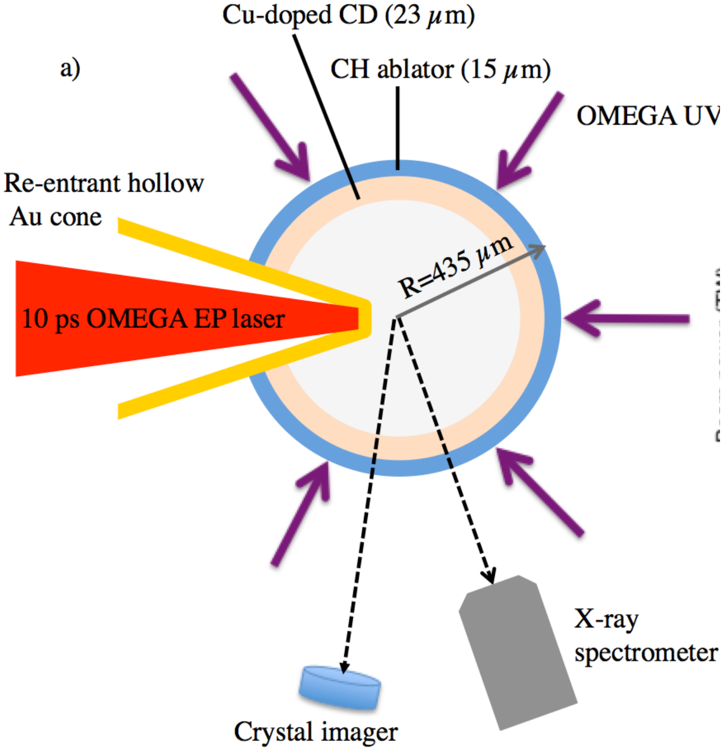

- Cu-doped CD shell has similar outer diameter and same mass as previous FI CD shell
- Characterize EP beam produced fast electron transport with Cu K-shell diagnostics:
  - Cu Kα x-ray yield and spatial distribution by a calibrated x-ray spectrometer(ZVH) and a spherical crystal imager (SCI)

Comparison of SCI from OMEGA-only vs. Joint shots shows spatial distribution of OMEGA EP produced Kα

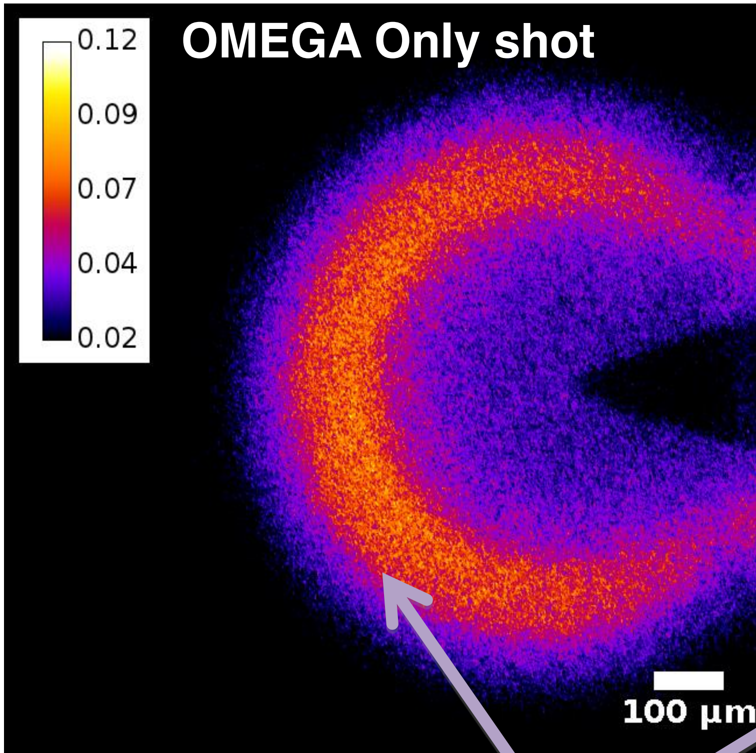

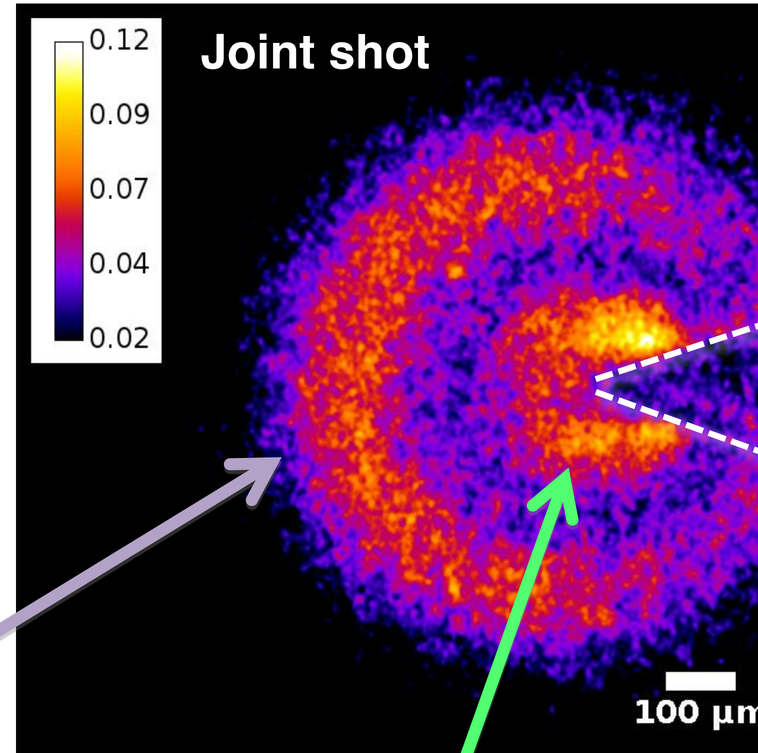

- Cu Kα from in-flight shell produced from suprathermal electrons induced by OMEGA
- Cu Kα from fast electrons induced by OMEGA-EP in the imploded core

Measured Kα distribution agrees with density profile predicted by 2D rad-hydro code DRACO

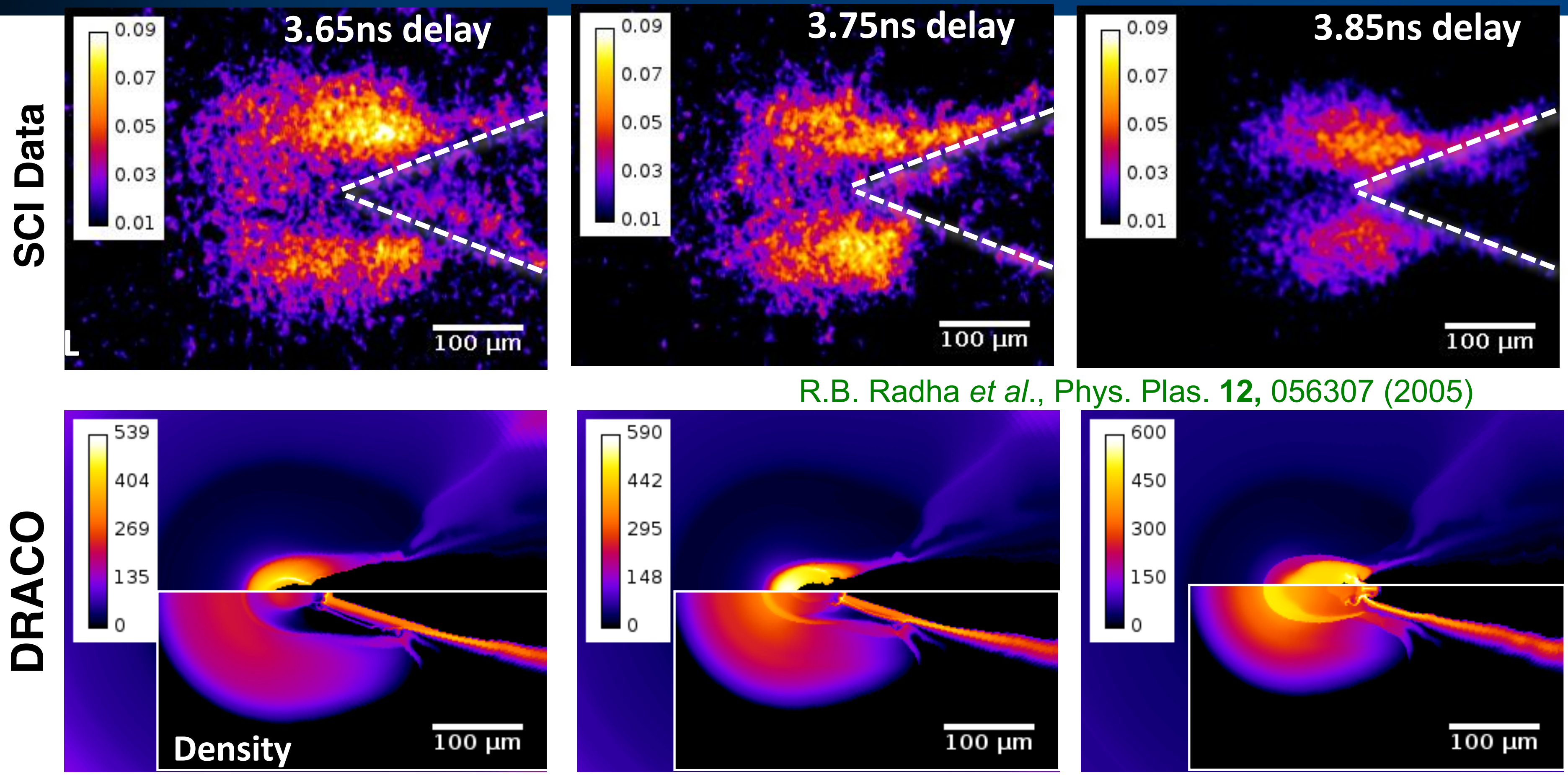

R.B. Radha *et al.*, Phys. Plas. **12,** 056307 (2005)

- Strong correlation of Cu Kα source position with DRACO simulated density
- Cu Kα produced as far back as 100um from cone tip
- Reduction in Kα signal at cone tip is partially due to heating of the core thereby shifting Cu Kα line out of imaging crystal bandwidth

LSP simulations to characterize 10ps laser-plasma interaction and fast electron source for both low- and high- contrast cases

Plasma setup: HYDRA simulation calculated the preplasma conditions (OMEGA EP prepulse), which were initialized into LSP to simulate the LPI including field ionization.

Low-contrast (21mJ,3 ns)

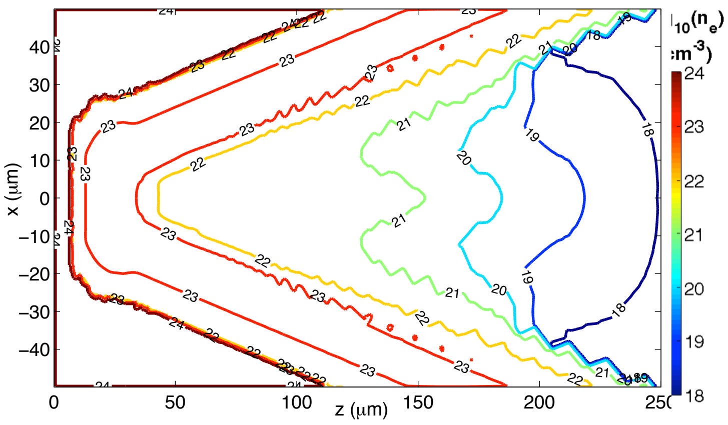

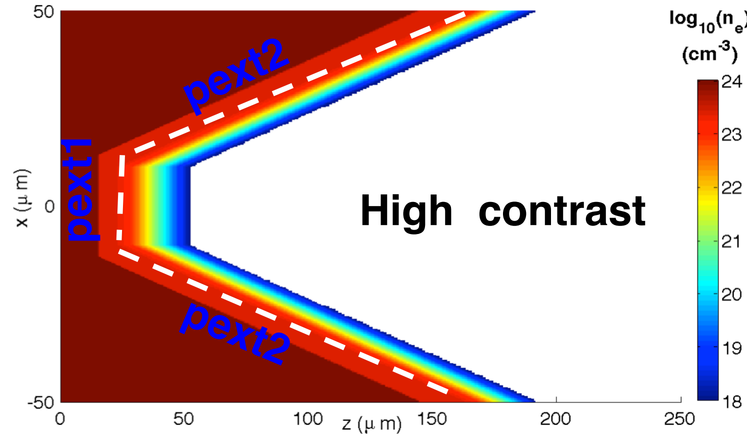

High-contrast (<1mJ) L=2μm is assumed

(pext* : extraction plane to diagnose time-integrated hot electron source though the cone tip and wall)

Laser setup: EP 10ps laser focal spot spatial and temporal distributions are fitted well in the simulation.

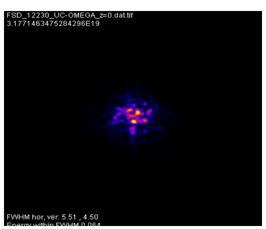

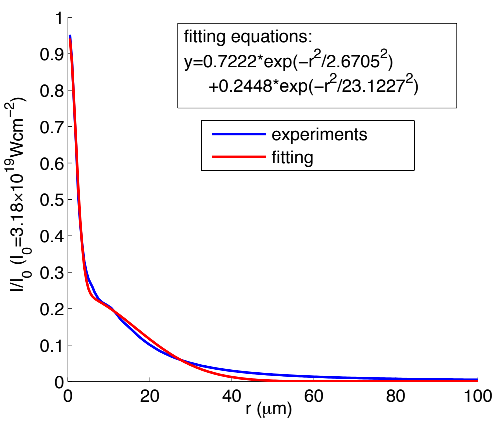

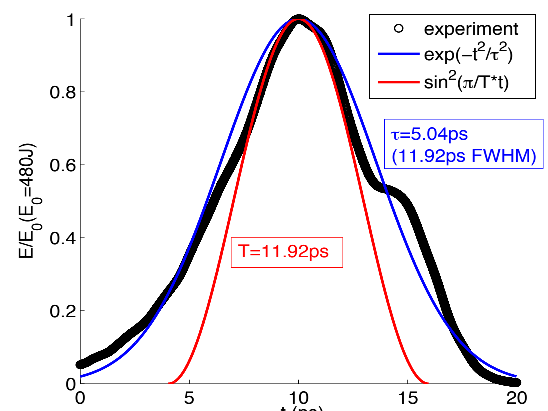

Complex laser filamentation and strong magnetic field generation defines LPI in two cases

Poynting flux (t=6.4ps)

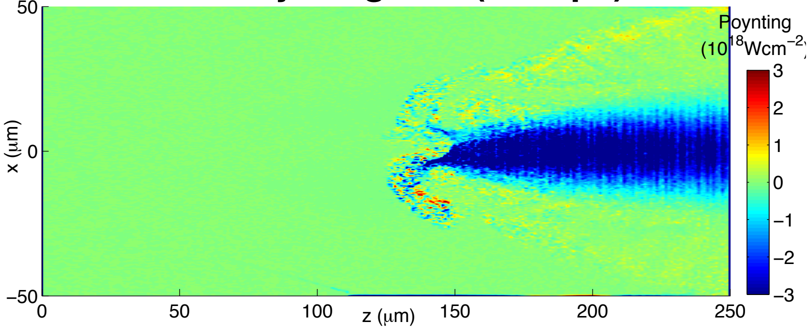

Poynting flux (t=6.4ps)

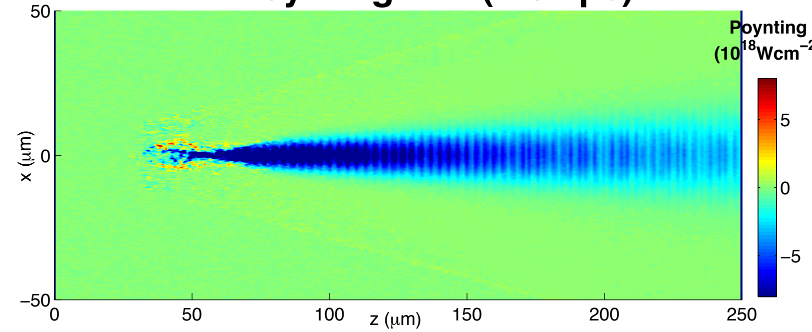

Quasistatic azimuthal magnetic field (t=6.4ps)

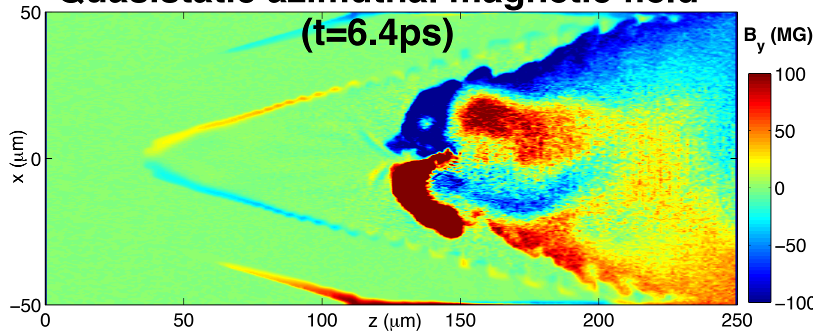

Quasistatic azimuthal magnetic field (t=6.4ps)

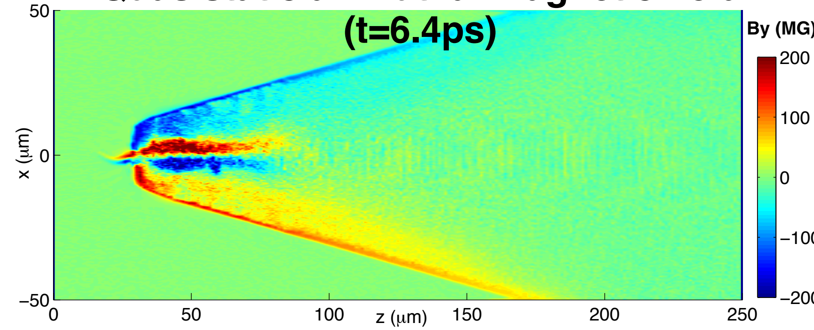

e- energy density (t=6.4ps)

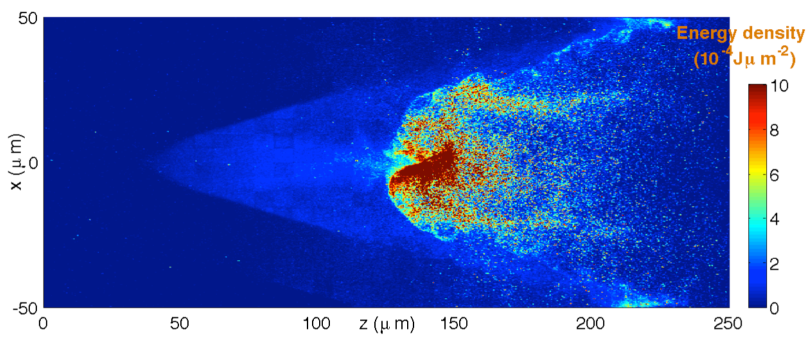

e- energy density (t=6.4ps)

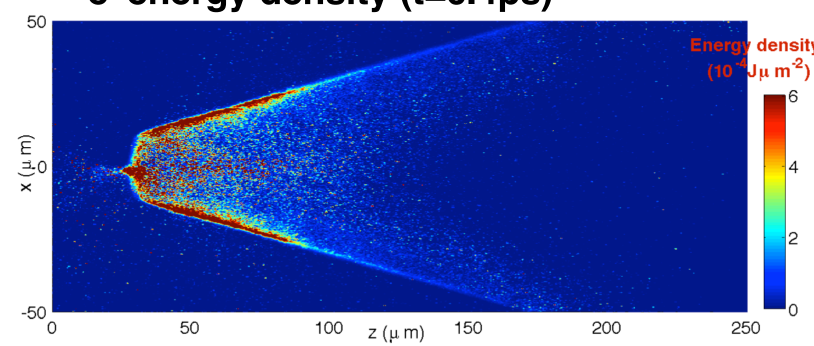

High contrast significantly improved the coupling efficiency from laser to fast electrons that enter into the cone

Laser energy in simulation : 320J

Low contrast

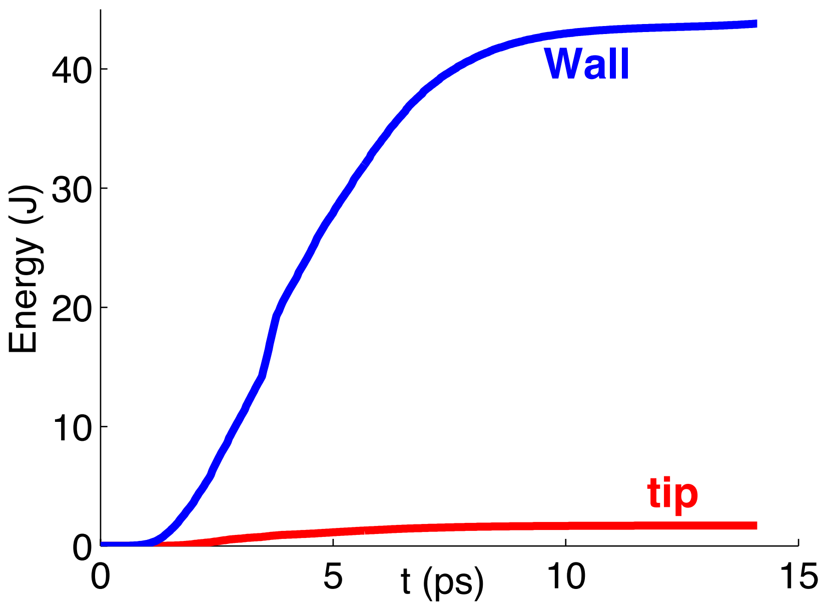

High contrast

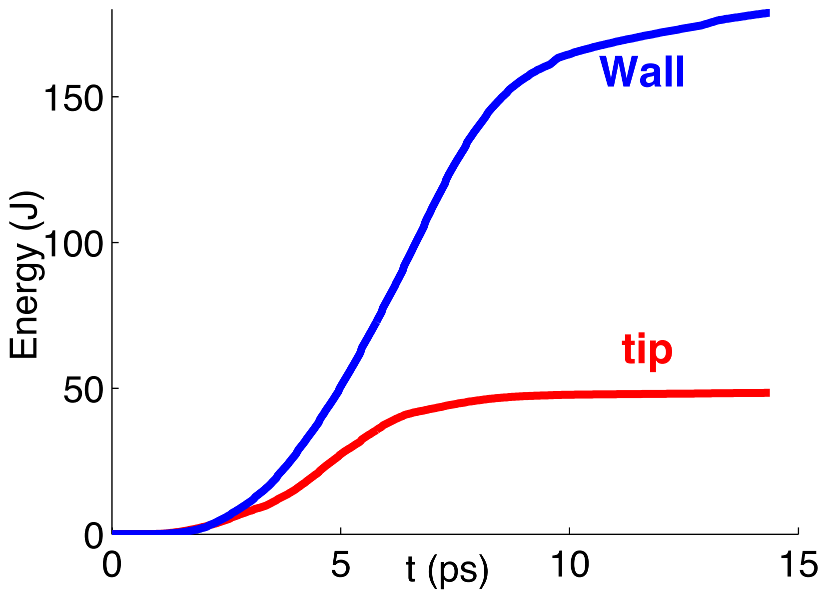

14% of laser energy coupled to fast electrons that enter into cone (wall and tip), among which:

- **13% reach the side walls**
- **~1% reach the cone tip**

65% of laser energy coupled to fast electrons that enter into cone (wall and tip), among which:

- **45% reach the side walls**
- **~20% reach the cone tip**

LSP simulations with the PIC simulated electron energy spectrum captures features observed in experiments

A.A. Solodov, LLE

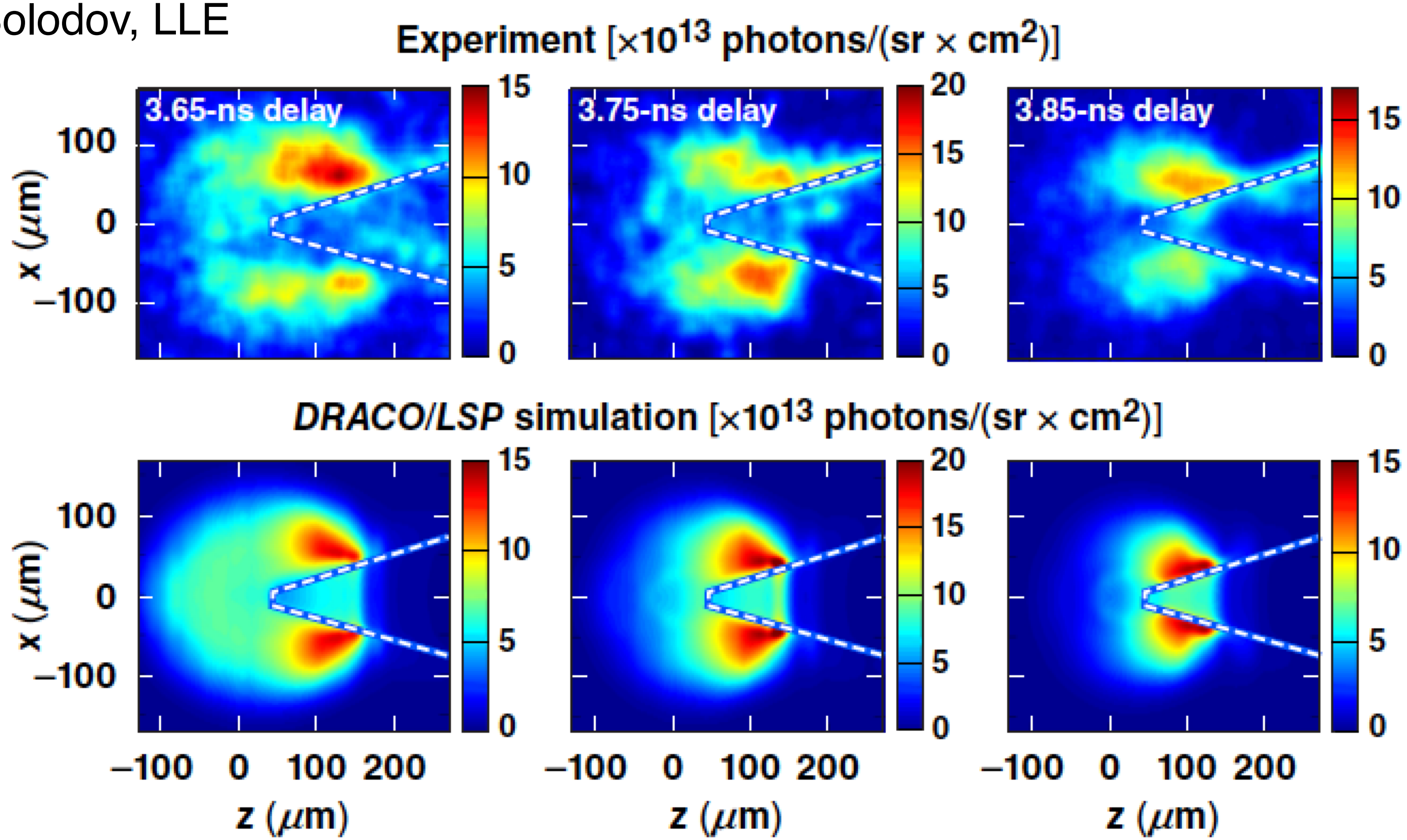

- Two-temperature energy spectrum (T_1=0.3 MeV, T_2=4 MeV)
- Isotropic fast-electron angular distribution
- Injected ~100 μm back from the tip
- Some differences can be because of 3D effects and target imperfection

Large distance from source to the core and divergence explains the low energy coupling to the core

A.A. Solodov, LLE

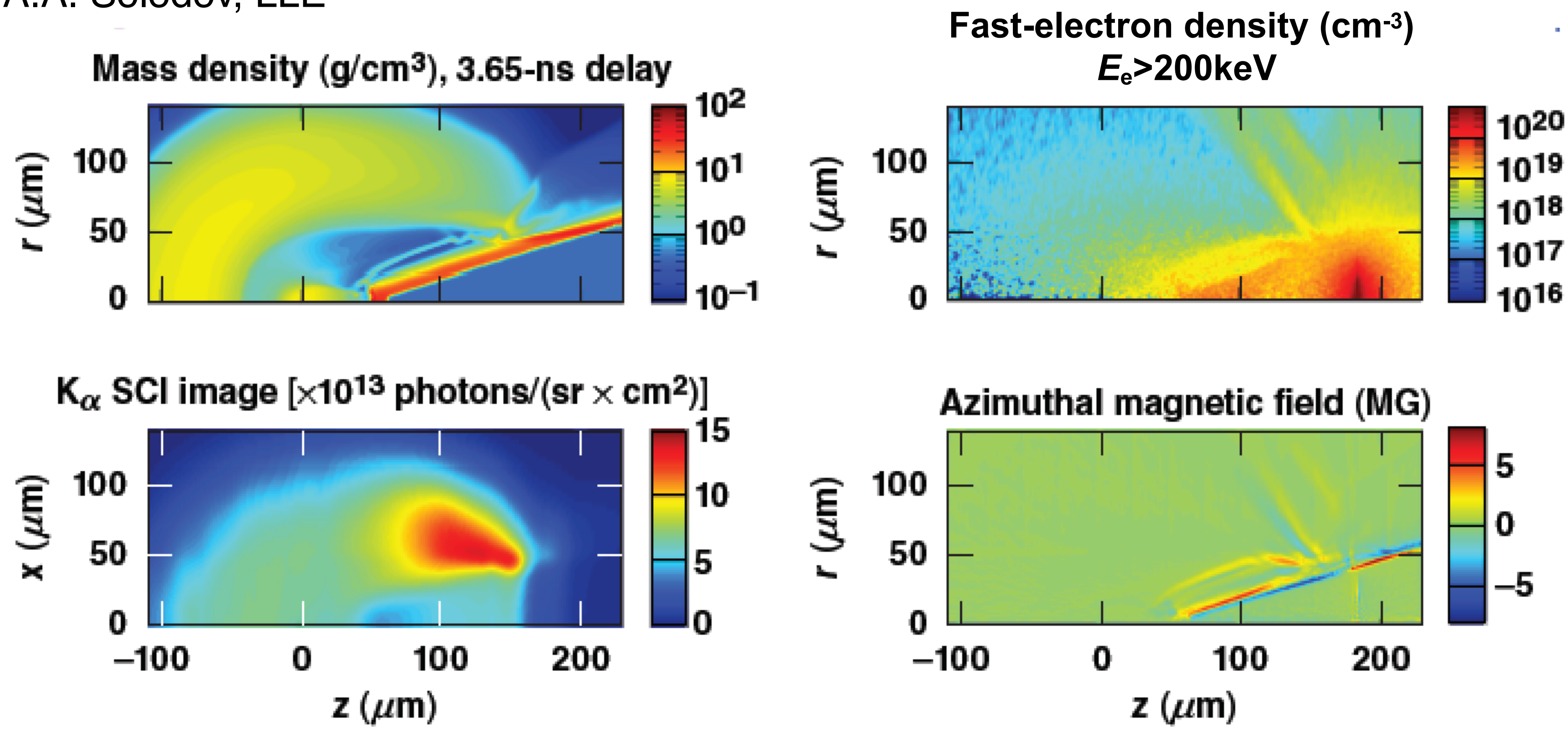

- About 3.8 % of the total fast-electron energy is coupled to the core ($\rho_{CD} > 1$ g/cm^3)
- Large distance from the source to the core
- Large divergence

ZUMA simulated Kα spatial distribution is in good agreement with experimentally measured values

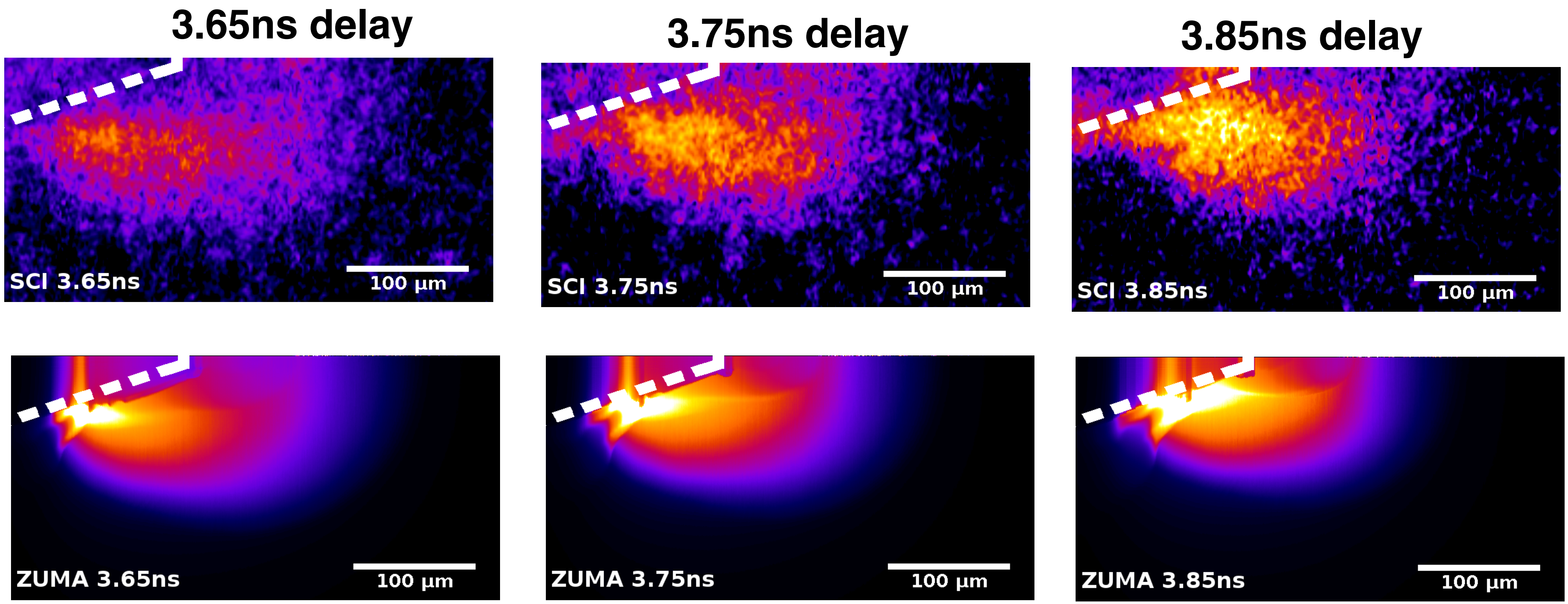

C. Jarrott, Physics of Plasmas (in preparation)

- **Source is injected 100 μm from cone tip**
- **Source divergence 50°**
- **Lack of Ka signal at cone tip seen in temperature corrected ZUMA output**

Optimizing target and implosion to form a denser core* to facilitate fast electron energy coupling

*W. Theobald, A.A. Solodov et al., Nature Communications 5, 5785 (2014)

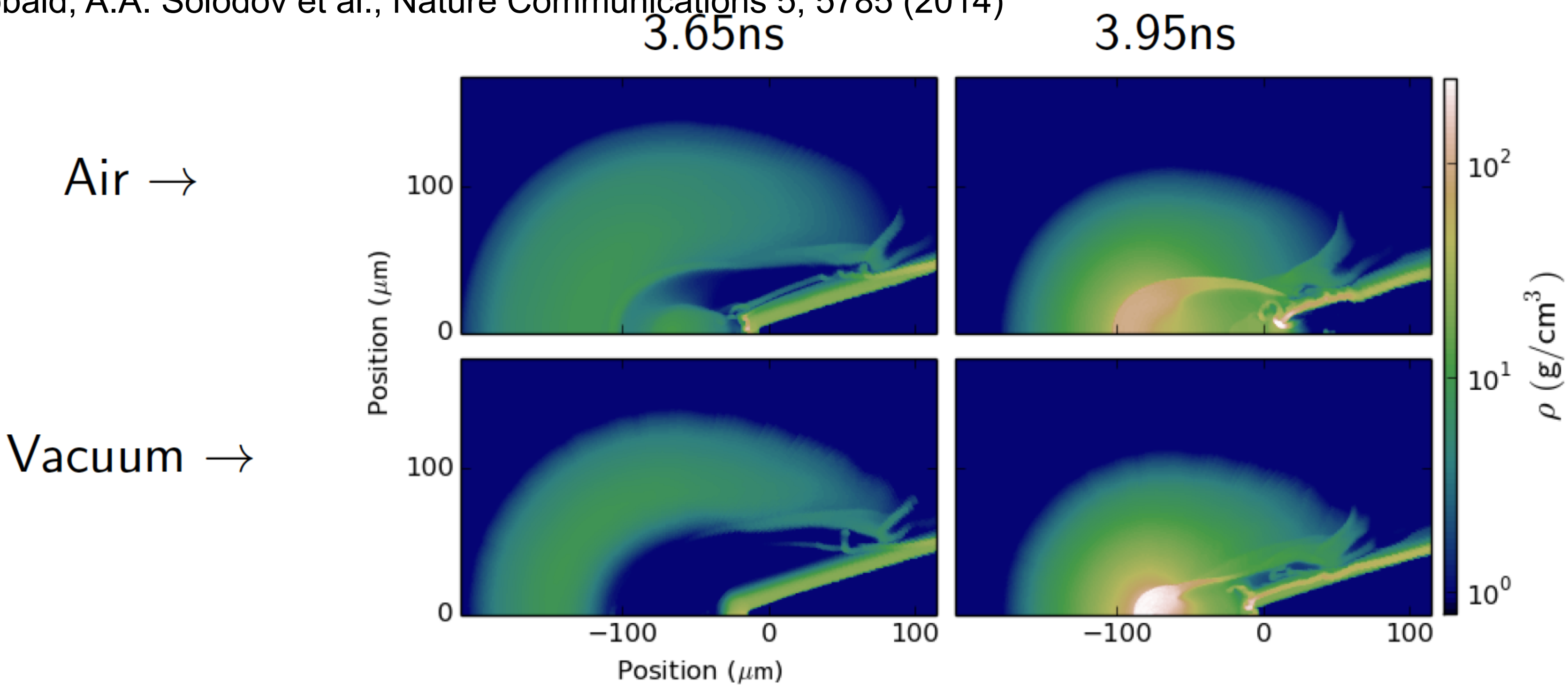

Gas pressure	ρR_{break} (mg/cm^2)	ρR_{max} (mg/cm^2)
0.8-atm air	80	300
Vacuum	360	600

- **DRACO simulations of implosion with a vacuum shell shows a much delayed cone-tip breakout time and a significant increase in ρR**

Enhanced energy coupling in optimized experiments with 40-um tip cone and vacuum shell

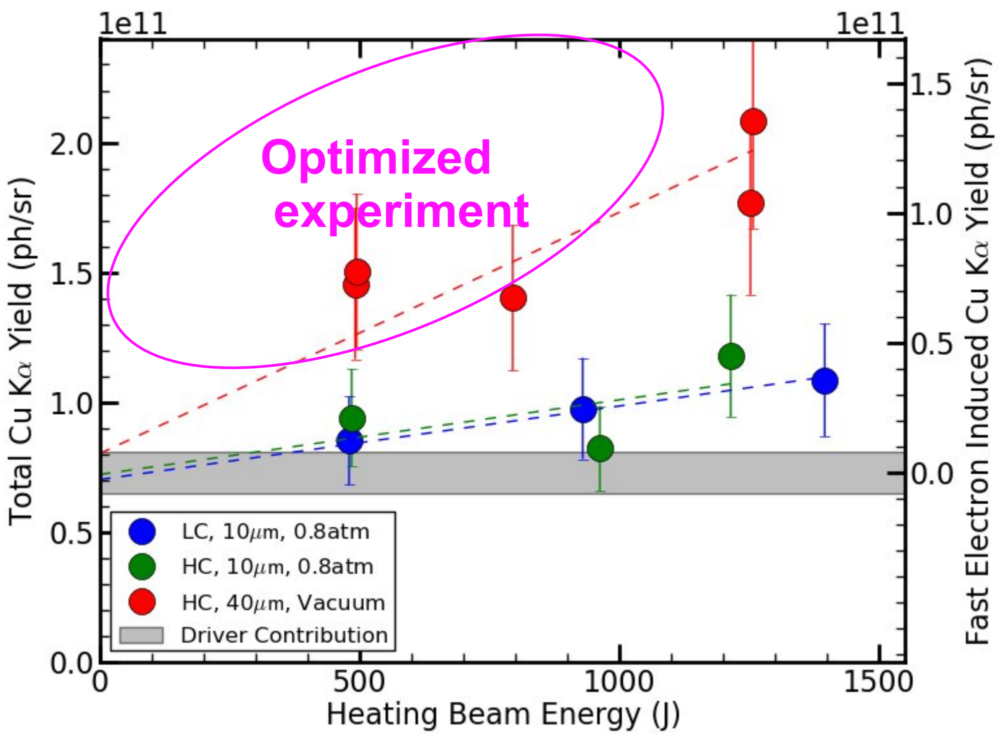

L.C. Jarrott, **Nature Physics (2016)**

- **4X increase in the observed Kα yield and up to 7% laser energy is coupled to the compressed plasma in the optimized experiment**
  - **A denser core stops electrons more effectively**
- **Cu Kα is emitted closer to the cone tip**
- **40 μm tip mitigates preplasma facilitating energy deposition at the tip**

New methods are warranted to mitigate electron divergence

Outline

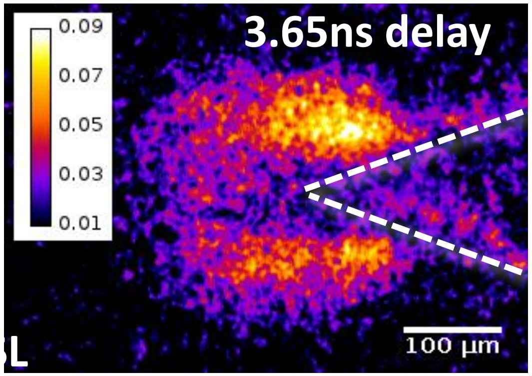

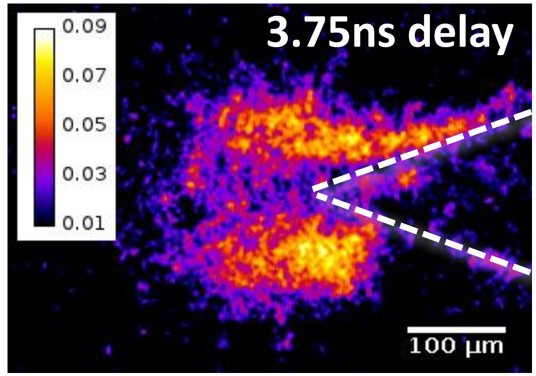

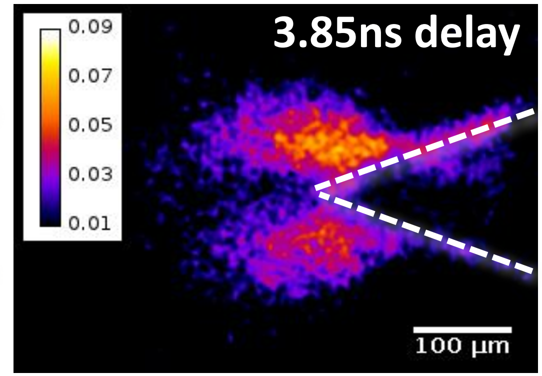

CH Plasma
30 mg/cm^3
360 µm

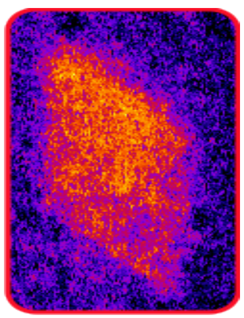

Cold CH
Solid1 g/cm^3
50 µm

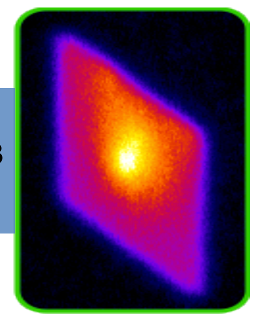

Cold CH
Foam
200 mg/cm^3
250 µm

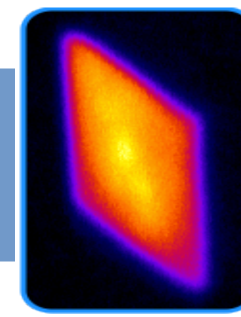

Un-driven HDC

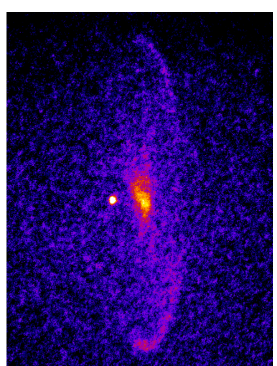

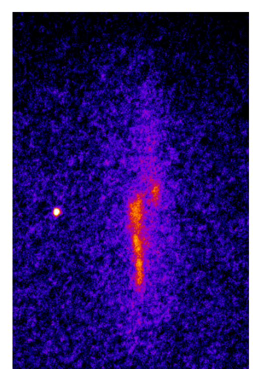

Un-driven VC

Al doped foam target was developed to create and characterize large volume plasma

Schematic Design of Foam Package Target

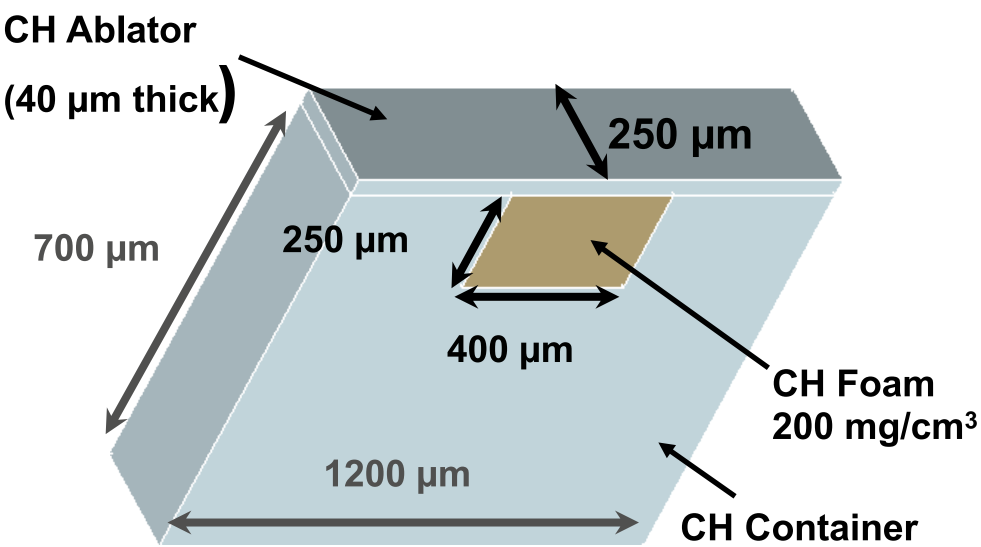

X-ray Radiograph of Target

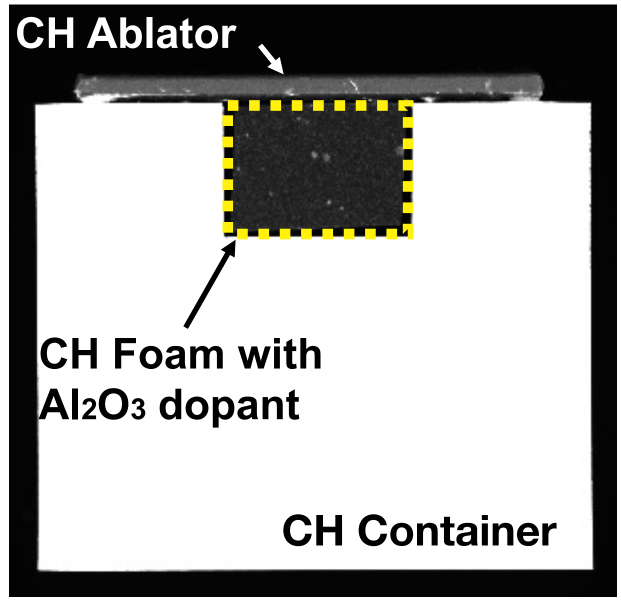

Al atomic density is ~2-3% of CH atomic density.

- **Al doped CH foam (200 mg/cm^3) in a plastic container with Al doping of 2-3% of CH atomic density**

Shock heated foam target was characterized with x-ray line absorption spectroscopy

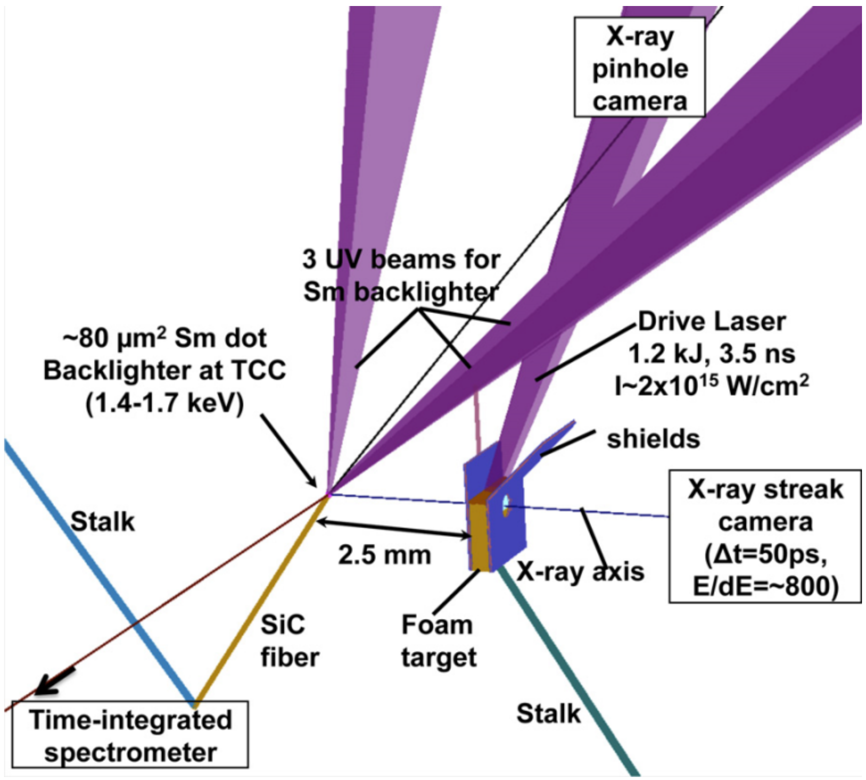

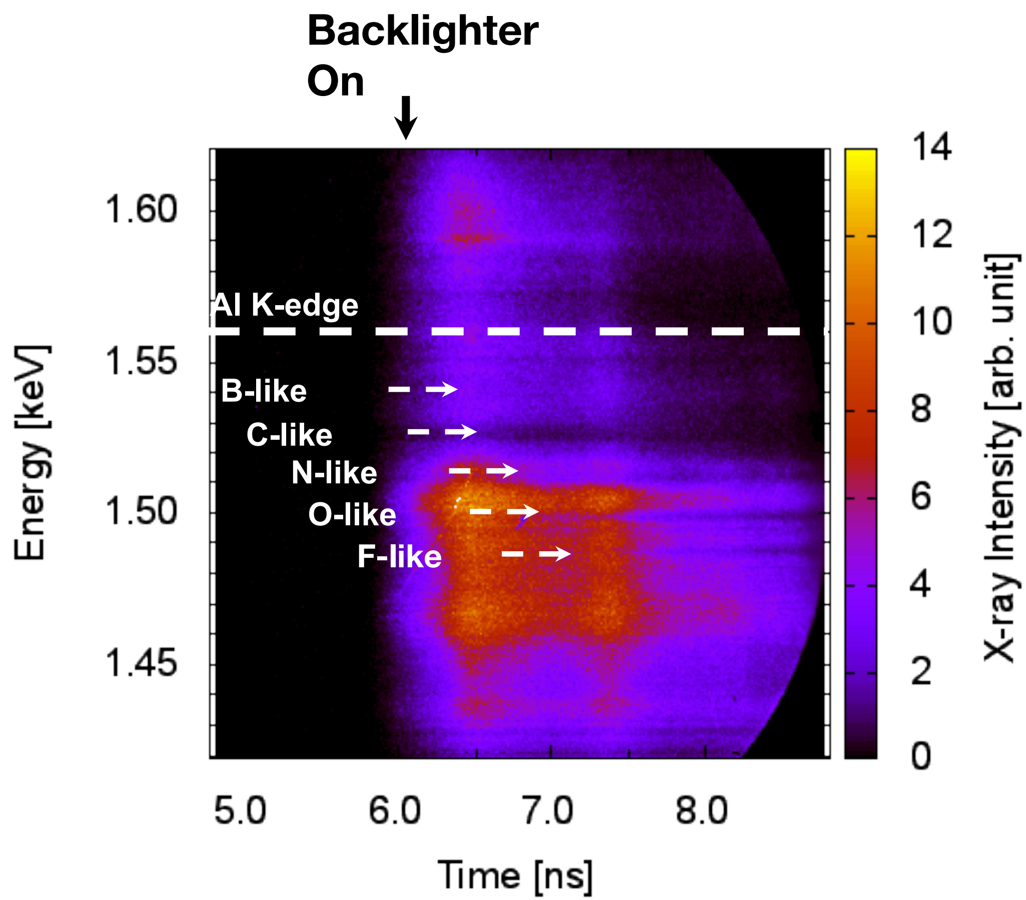

- Sm backlighter was used for absorption spectroscopy
- Al 1s-2p line absorption was observed with streaked x-ray spectrometer.

H. Sawada et al. , High Energy Density Physics 8,180-183 (2012).

Temperature and density were inferred to be 40 ± 5 eV and 30 ± 10 mg/cm³ respectively at 7 ns

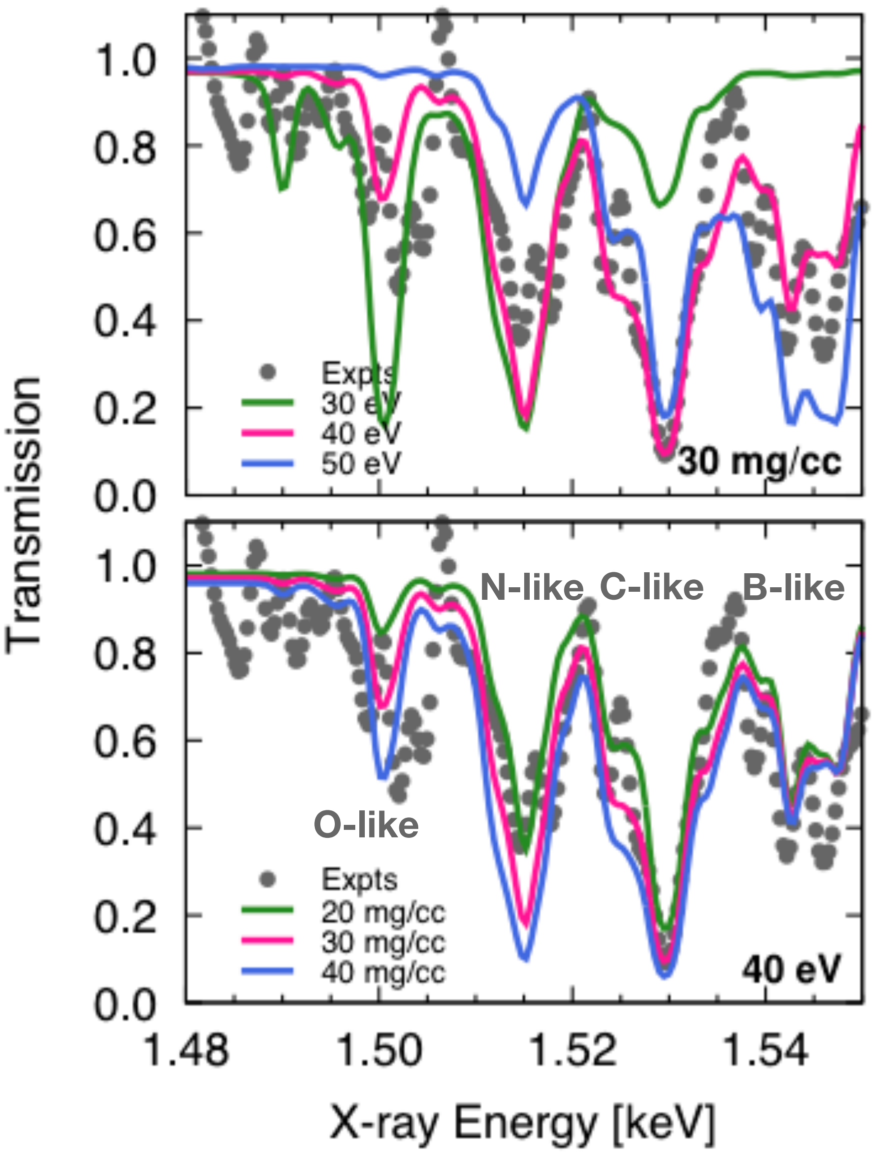

- **PrismSPECT† was used to estimate plasma characteristics averaged along the line of sight.**
- **Fitting is sensitive to Te, but could have relatively large uncertainty in density.**

T. Yabuuchi et al., Phys. Plasmas 19, 092705 (2012).

Diffused and diverged X-ray emission was observed in driven targets

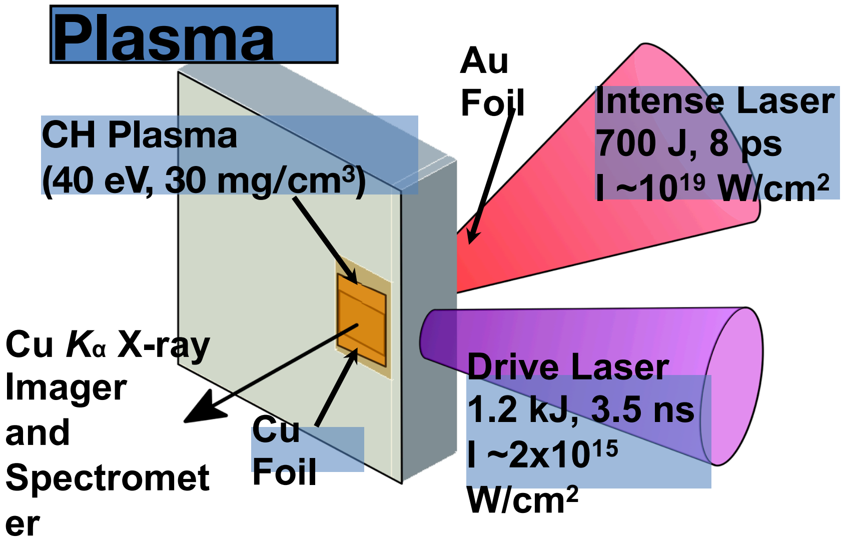

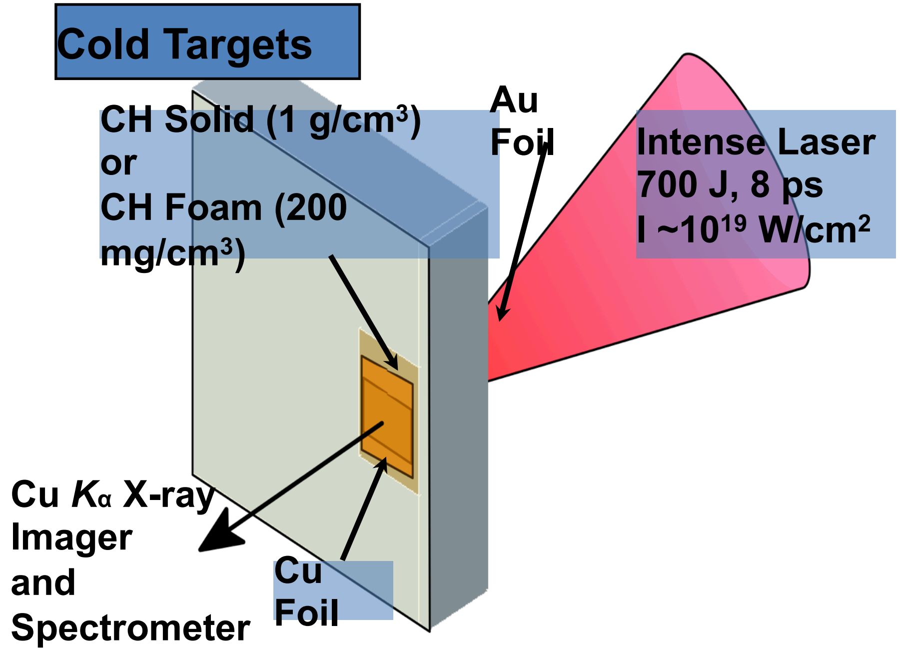

CH Plasma
30 mg/cm³
360 μm

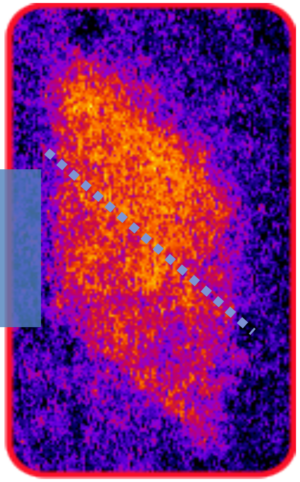

Cold CH Solid
1 g/cm³
50 μm

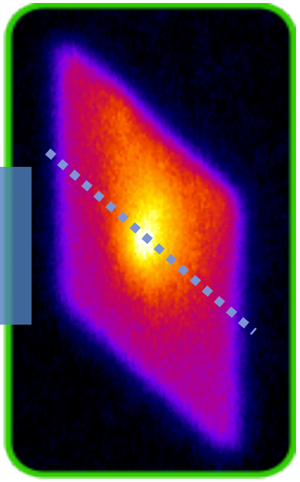

Cold CH Foam
200 mg/cm³
250 μm

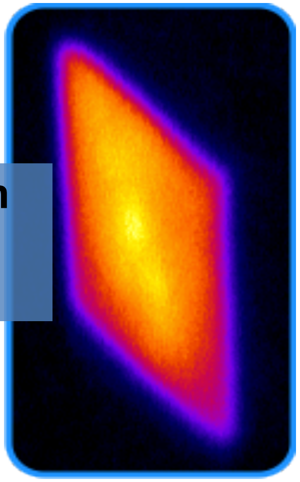

Weaker Kα signal was observed with plasma target

Line Out of Cu *K*α x-ray Emission (Imager)

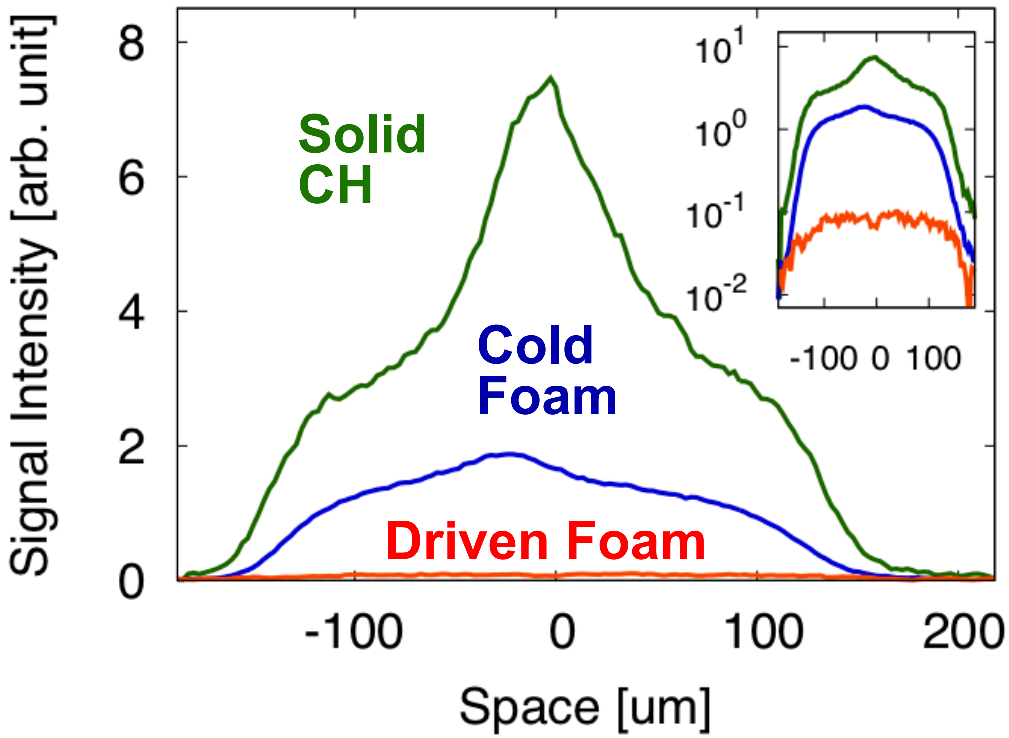

Integrated Cu *K*α x-ray signal (Spectrometer)

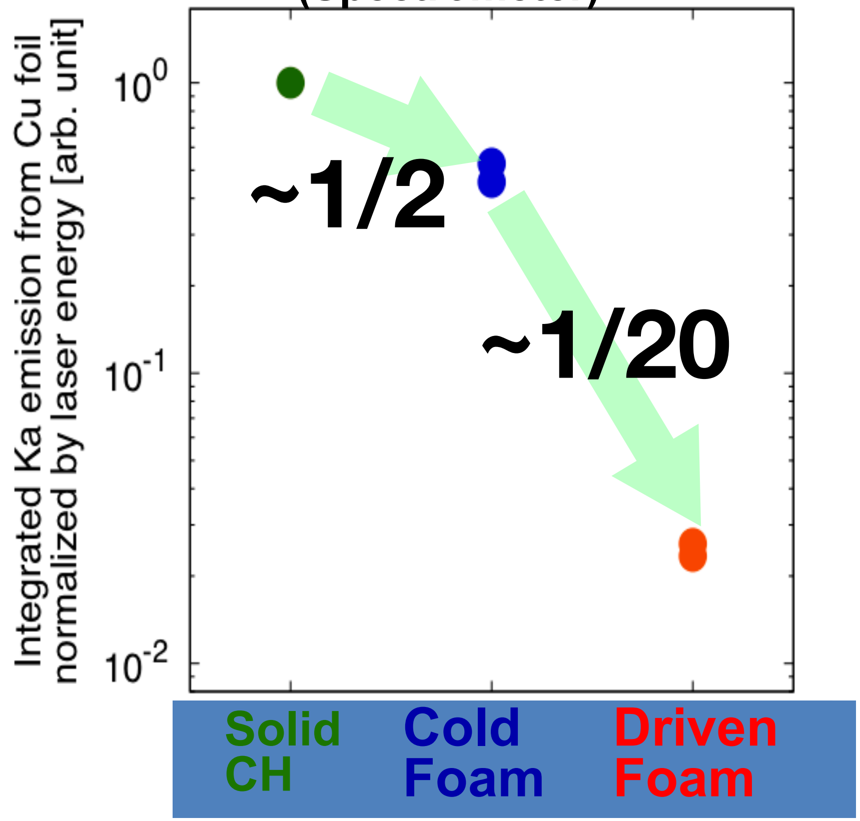

- **Almost uniform *K*α emission was observed with plasma, which suggests a largely diverged fast electron beam.**

Simulation show density of the` plasma and collisions affect the fast electron transport

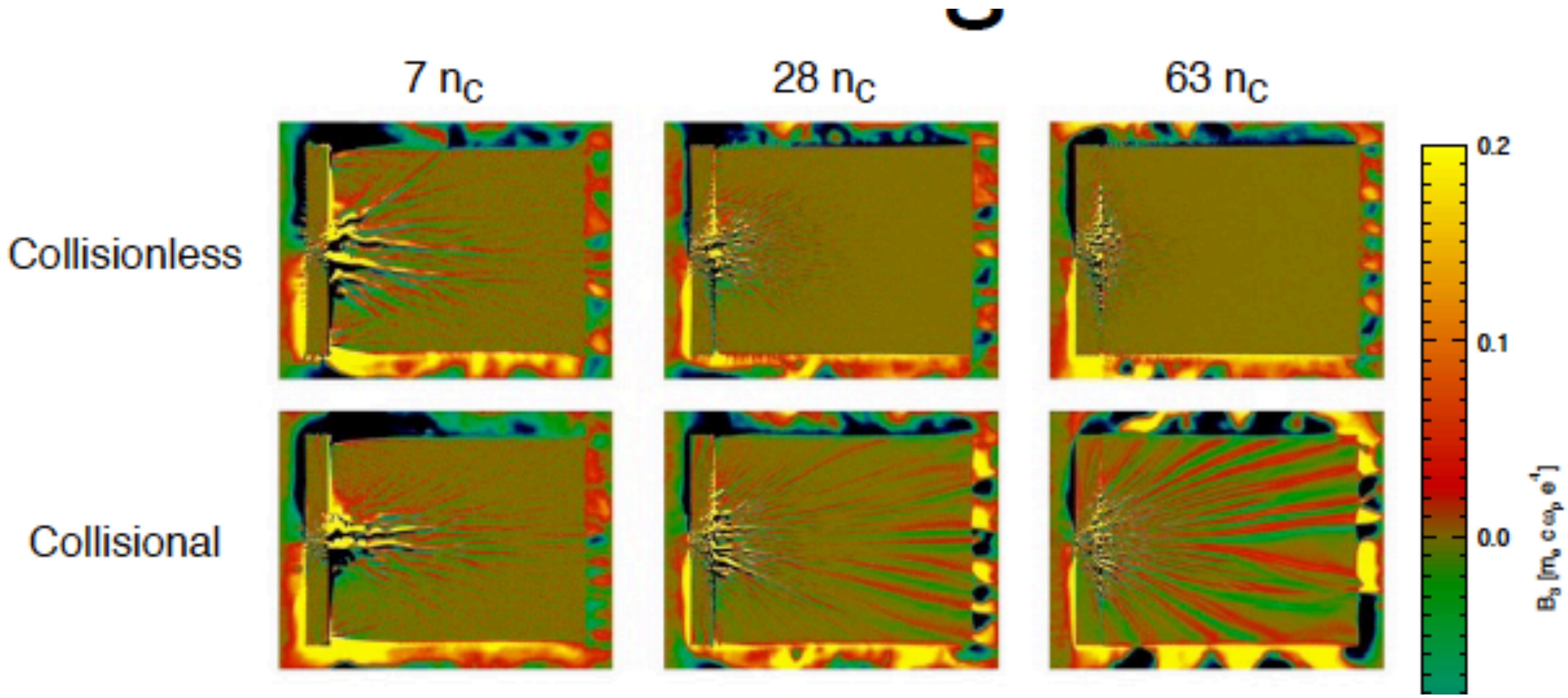

- **Collisions make a significant difference in electron beam propagation**

J. May, Warren Mori, UCLA

Simulation show density of the` plasma and collisions affect the fast electron transport

J. May, Warren Mori, UCLA

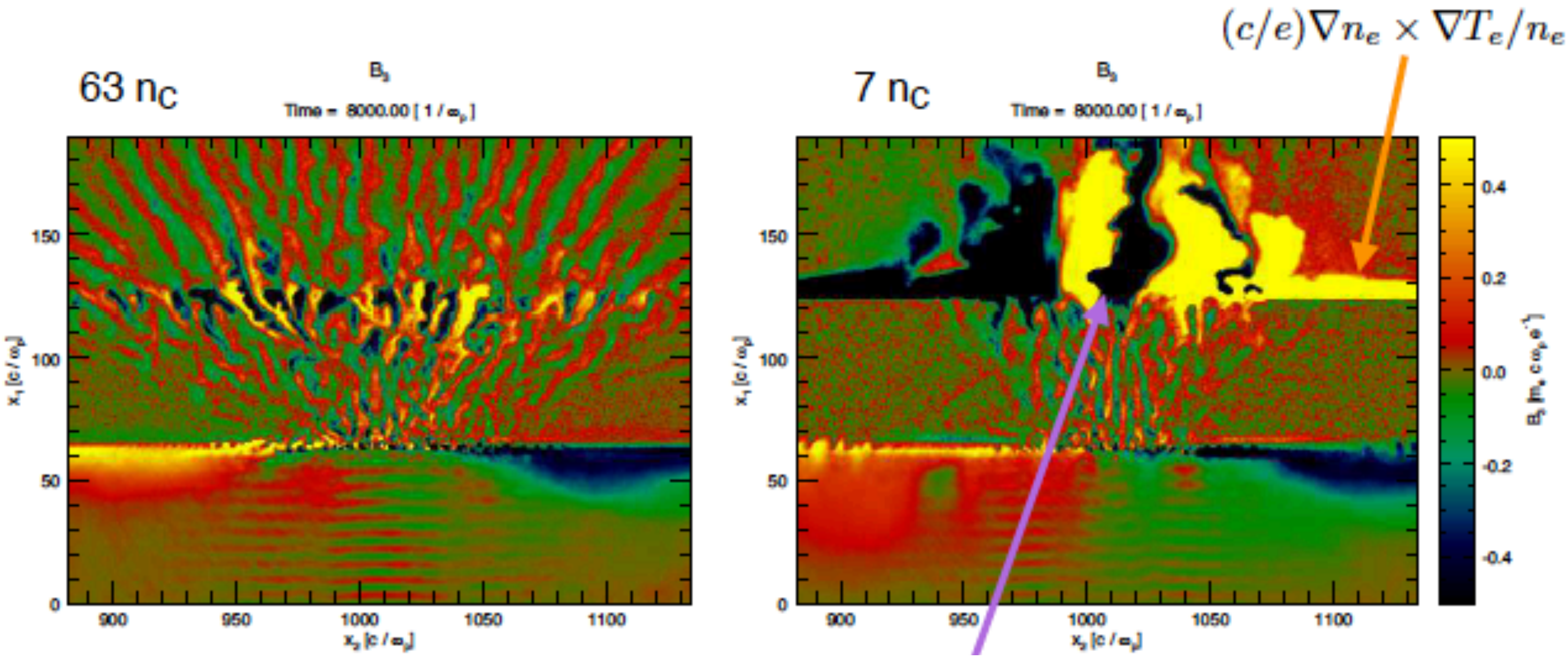

- **Significant magnetic fields are generated at the interface which inhibit fast electrons**

Outline

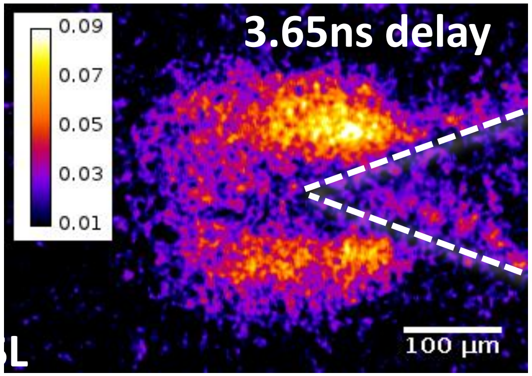

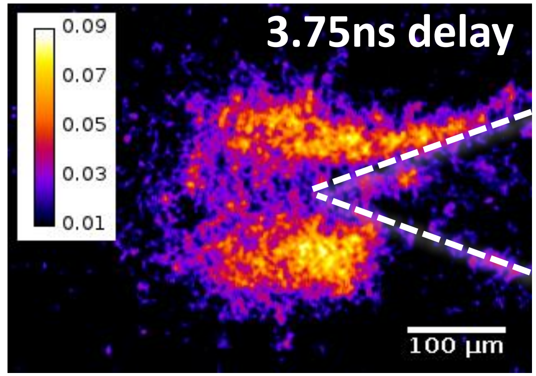

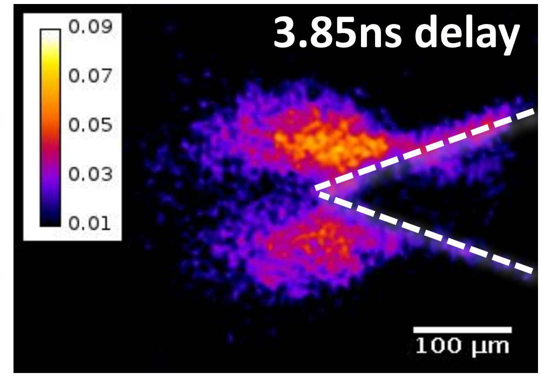

CH Plasma
30 mg/cm^3
360 μm

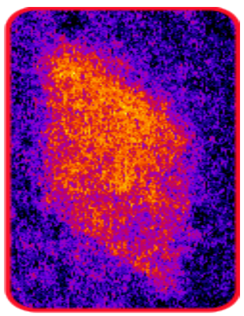

Cold CH
Solid1 g/cm^3
50 μm

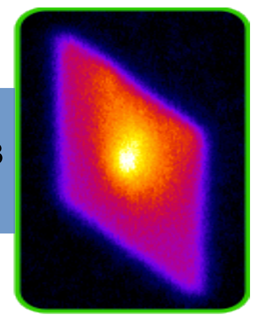

Cold CH
Foam
200 mg/cm^3
250 μm

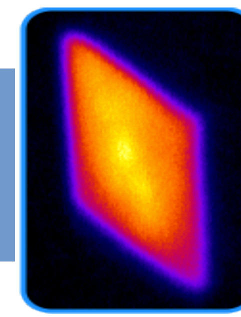

Un-driven HDC

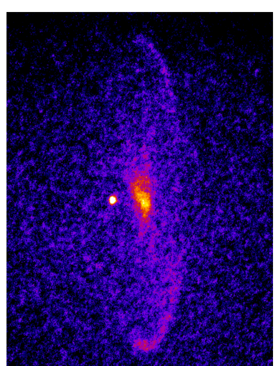

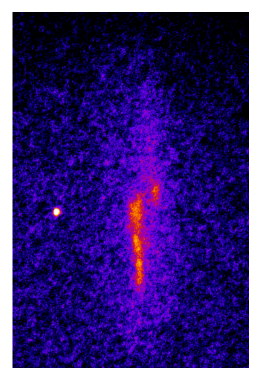

Un-driven VC

Electron transport through altropes of carbon

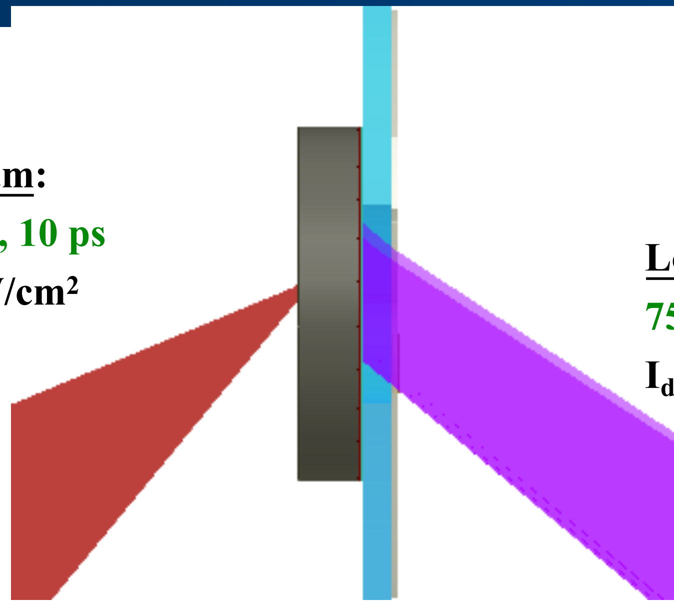

Target schematics:
Not to scale

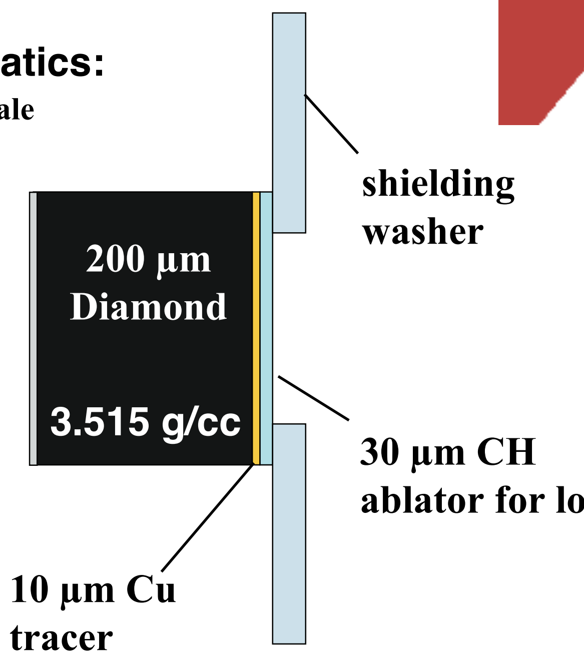

Two target types:
- preserve ρR

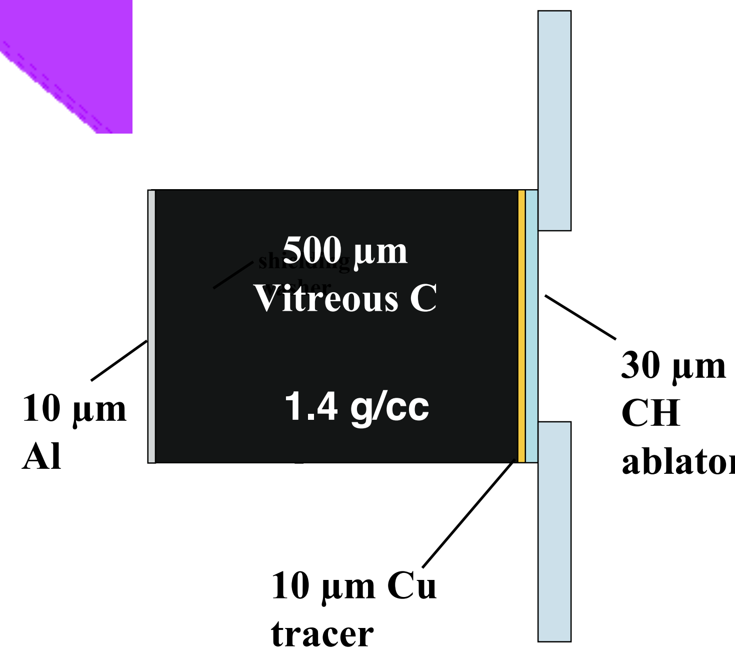

Electron beam transport in allotropes of carbon is different

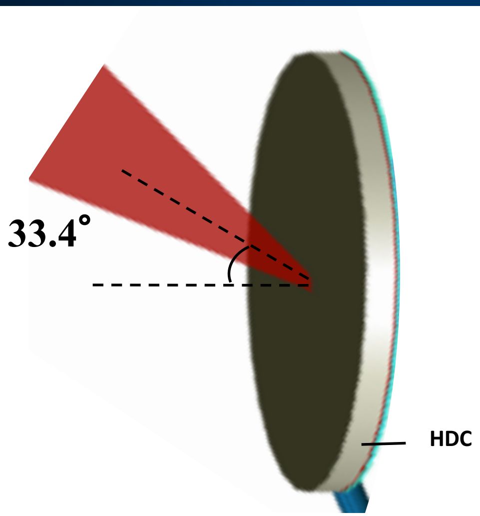

Imager field of view reference

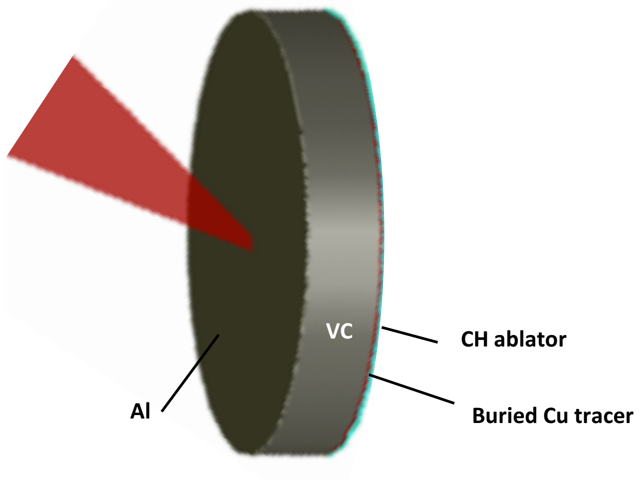

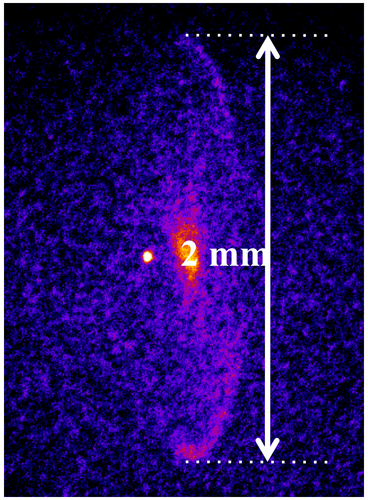

- Data shows high divergence of electrons interacting with Cu (opening angle~49degrees)
- Evidence of recirculation in HDC as edges fluoresce
- Signal indicates filamentation through VC target.

Un-driven VC

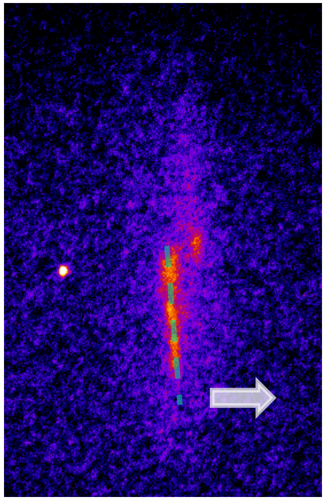

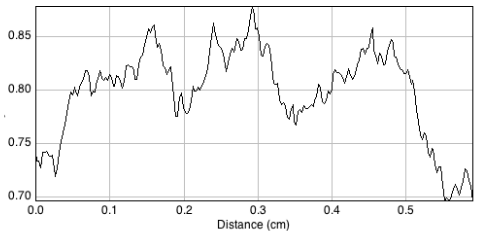

Summary

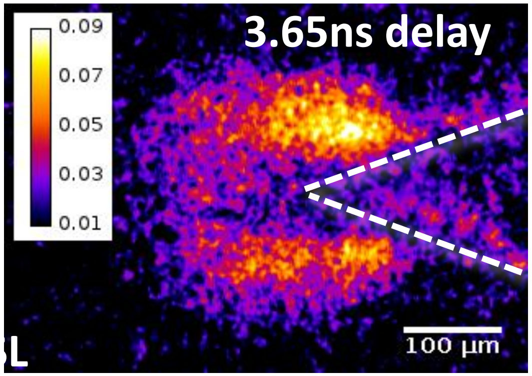

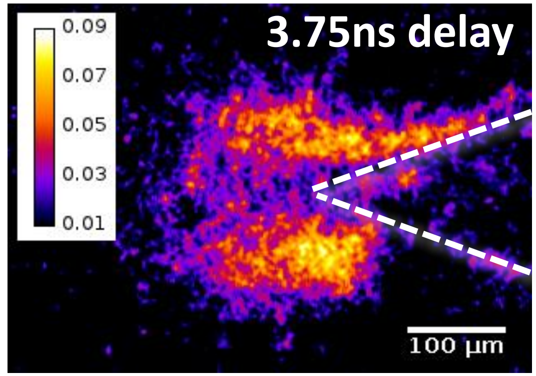

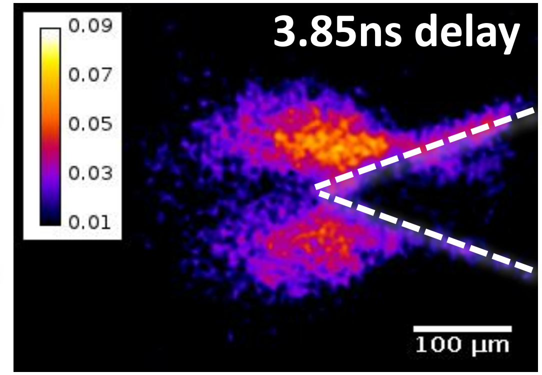

CH Plasma
30 mg/cm^3
360 µm

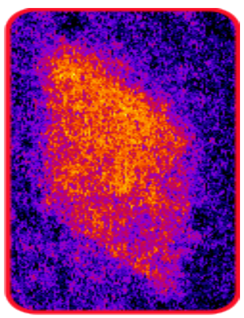

Cold CH
Solid1 g/cm^3
50 µm

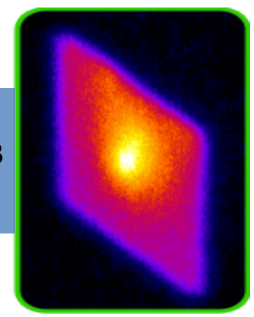

Cold CH
Foam
200 mg/cm^3
250 µm

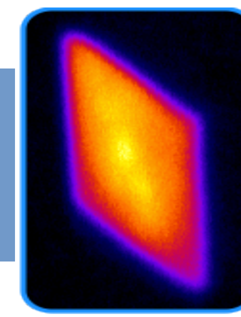

Un-driven HDC

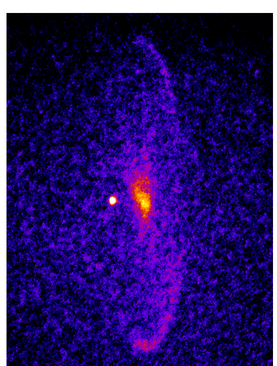

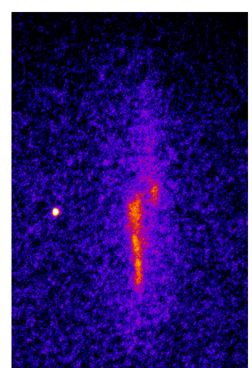

Un-driven VC